Forest Ecology and Management 411 (2018) 46–66

Contents lists available at ScienceDirect

Forest Ecology and Management

journal homepage: www.elsevier.com/locate/foreco

From young to adult trees: How spatial patterns of plants with different life strategies change during age development in an old-growth Korean pine-broadleaved forest

Alexander Omelko[a,*], Olga Ukhvatkina[a], Alexander Zhmerenetsky[a], Lidiya Sibirina[a], Tatyana Petrenko[a,b], Maxim Bobrovsky[c]

[a] *Federal Scientific Center of the East Asia Terrestrial Biodiversity FEB RAS, 100 let Vladivostoku Str. 159, Vladivostok 690022, Russia*
[b] *Far Eastern Federal University, Sukhanova 8, Vladivostok 690950, Russia*
[c] *Institute of Physicochemical and Biological Problems of Soil Science, Institutskaya Str., 2, Pushino 142290, Russia*

ARTICLE INFO

Keywords:
Point pattern
Recruits
Old-growth
Life strategy
Korean pine
Temperate forest

ABSTRACT

We used point pattern analysis (pair-correlation function, $K2$ function, distance to kth neighbor D_k, and spherical contact distribution function H_s) to describe the process of plant pattern formation for five dominant tree species with different life strategies in a mixed-forest stand with Korean pine (*Pinus koraiensis* Sieb. et. Zucc.) in the southern part of the Sikhote-Alin mountain range (southeastern Russia). We subdivided each species pattern using an ontogenetic classification of individuals: immature, virginal, and generative. We also analyzed stump pattern structure, which marks canopy gap formation locations in recent decades. We also studied the shade tolerance changes of pre-generative plants during their development. As a result, we found similarities between the processes of pattern transformation for the different species. Namely, they transform from pronounced aggregated distributions of plants at several spatial scales (immature plants) to a random pattern (middle-aged and old generative plants). This transformation of pattern structure occurs because the immature plants accumulate under a canopy and require significantly improved light conditions that can only be found in gaps to transition into the virginal and young-generative stage. In turn, the process of gap formation is stochastic, and the stand is characterized by a low-intensity disturbance regime. Thus, the pre-generative plant patterns are filtered by randomly formed gaps, and thus only individual randomly distributed plants reach the middle-aged and old generative ontogenetic states.

1. Introduction

The study of spatial and temporal patterns of plants is crucially important for solving a wide range of ecological problems connected to community dynamics, the coexistence of species and biodiversity maintenance (e.g., Chesson, 2000; Wright, 2002; Brown et al., 2011; May et al., 2015). Community spatial pattern is the result of plant interactions with each other and the environment (e.g., Harms et al., 2001; John et al., 2007; Lai et al., 2009; Zhang et al., 2010a, 2010b). However, it also presents the peculiarities linked to species life-strategies such as seed spreading strategies and the maximal distance of their distribution, shade-tolerance, plant lifetimes, and sizes (Brzeziecki and Kienast, 1994; East-European Forests (Russia), 2004). By studying the spatial pattern of the species in a stand, we can better understand its life-strategy traits (Seidler and Plotkin, 2006; Jara-Guerrero et al., 2015). Comparisons of the features of different species' patterns provide clues for understanding how life strategy features are expressed and thus which life-strategy traits differ and which are similar. Finally, considering the formation of different species' patterns all together, we can make conclusions regarding the formation of community spatial structures.

The processes leading to some kinds of patterns differ in duration depending on plant lifetime and development peculiarities. The formation of patterns by trees may last up to hundreds or even thousands of years (Smirnova, 2004). These patterns consist of plants that substantially differ in size, age and stages of development (Smirnova and Bobrovskii, 2001). Thus, for a meaningful analysis, we should divide tree patterns into functionally similar components, which is usually done by their heights (Hao et al., 2007), diameters (Liu et al., 2014; Punchi-Manage et al., 2014) or ages (Garcia-Cervigon et al., 2017). The

---

[*] Corresponding author.

E-mail addresses: omelko@biosoil.ru (A. Omelko), ukhvatkina@biosoil.ru (O. Ukhvatkina), zmerenetsky@mail.ru (A. Zhmerenetsky), sibirina@biosoil.ru (L. Sibirina), tanya232@mail.ru (T. Petrenko), maxim.bobrovsky@gmail.com (M. Bobrovsky).

https://doi.org/10.1016/j.foreco.2018.01.023
Received 18 September 2017; Received in revised form 11 January 2018; Accepted 13 January 2018

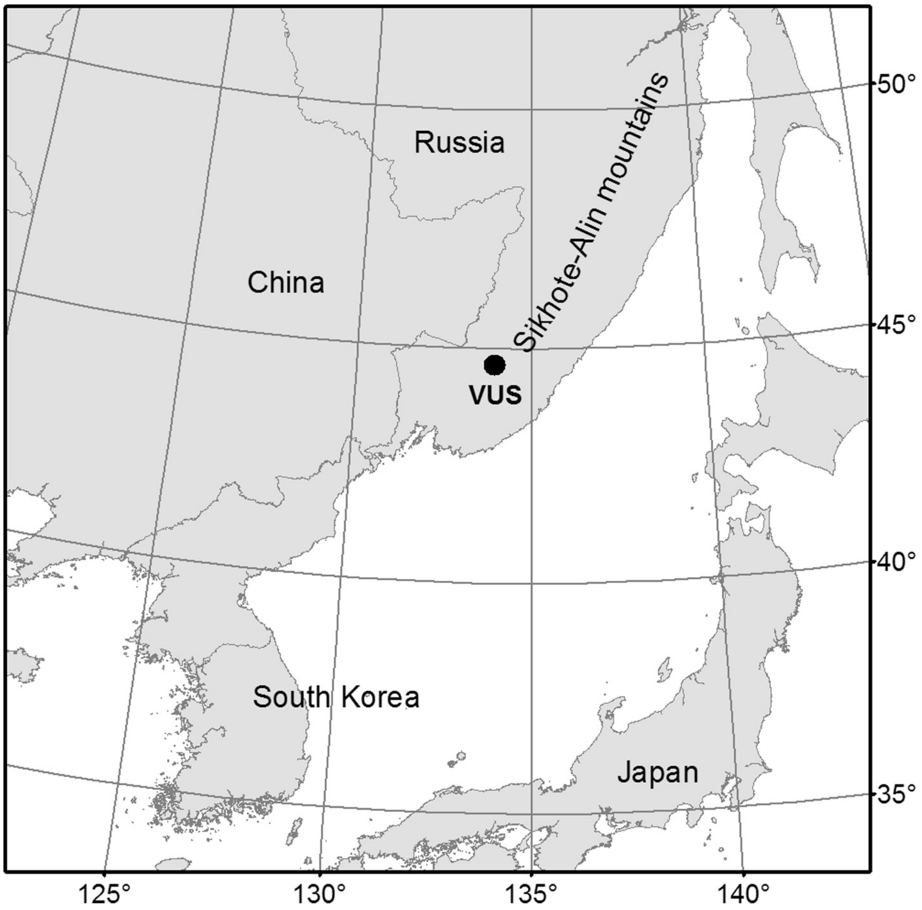

Fig. 1. Location of the study area on the Sikhote-Alin Mountains, South-Eastern Russia. VUS is Verkhneussyriysky Research Station of the FSC of Terrestrial Biodiversity FEB RAS.

Table 1
Characteristics of the dominant tree species.

Species	H_{max} (m)	DBH_{max} (cm)	A_{max} (years)	Shade tolerance	Life strategy
Abies nephrolepis	25	50	214	Shade tolerant	R-C
Betula costata	30	100	340	Light-demanding	R-C
Picea jezoensis	35	110	317	Shade-tolerant	C-S-R
Pinus koraiensis	42	150	527	Shade-tolerant	C
Tilia amurensis	30	100	250	Mid-tolerant	R-C

Note: H_{max} – maximum tree height (Usenko, 1968); DBH_{max} – maxium tree diameter at 1.3 m height (Usenko, 1968); A_{max} – maximum age (Petrenko et al., 2016; Omelko et al., 2016; Ukhvatkina and Omelko, 2016; Ukhvatkina et al., 2017). Life strategy (Grime 1979). Shade tolerance (Usenko 1968). Note that Wang et al. (2010) consider *T. amurensis* as shade-tolerant and *P. koraiensis* as a mid-tolerant species. In our opinion, such differences may be due to differences in the methods of determining shade tolerance.

concept of discrete descriptions of plant ontogenesis is promising for that purpose. In that concept, the populations of each species consist of sets of individuals at different stages of ontogeny development (East-European Forests (Russia), 2004). A similar approach is used to divide the individuals of populations when developing stage-structured matrix models (Caswell, 2001). The special feature of this approach is that although the individuals may differ in size and absolute age, they are at the same stage of ontogenetic development and play a similar role in a stand (Smirnova and Bobrovskii, 2001; Evstigneev and Korotkov, 2016). Using that concept, we can divide the population of any species into functionally homogeneous components – sets of plants at the same stage of ontogenetic development (East-European Forests (Russia), 2004) which, therefore, are under the influence of similar factors. Each of those components presents a certain stage of the stand dynamics. The pattern of such stages can be regarded as a snapshot of the process structuring the formation. By analyzing the snapshot, we can describe how it proceeds.

The object of our research are the Korean pine-broadleaved forests situated in north-eastern Asia, which are remnants of the Turgai flora that once existed across the entire territory of Eurasia (Krestov, 2003). These forests cover the southern part of the Russian Far-East, the north-eastern part of China, and parts of the Korean peninsula and Japanese islands (Krestov, 2003). The scarce land development in the Russian territory has contributed to the preservation of old-growth stands as well as unique sites that have not experienced human impacts and fires in the past 1500–2000 years (Omelko et al., 2016).

However, information on the structure and dynamics of those forests is fragmentary. The sparse materials presented in the literature on species ecological peculiarities (Usenko, 1968; Ishikawa et al., 1999; Orekhova, 2005; Komarova, 1986; Komarova and Trofimova, 2010; Komarova et al., 2010; Ukhvatkina et al., 2010) cannot fully characterize life strategy traits and the process of forest dynamics. Studies of mixed broadleaved-Korean pine forests conducted in north-eastern China (Zhang et al., 2008; Zhang et al., 2010a, 2010b; Wang et al., 2010; Liu et al., 2014) also cannot present a complete picture because of the considerable variability in climatic conditions and land development history; the described forests differ greatly from those studied in the stand structures and dominant species list.

For the detailed analysis of the patterns structure, it is necessary to use several summary statistics (Illian et al., 2008; Wiegand et al., 2013). These allow discerning whether the aggregation of plants was really due to plant-plant (i.e., interacting through their crowns or root

Table 2
General characteristics of plants at different ontogenetic stages.

Ontogenetic stage	Characteristic of plant
Germlings (*p*)	Mixed nutrition from the root and seed; there is a morphological connection with the seed and germinal structures
Juvenile (*j*)	Indicators and properties typical of an adult plant have not yet been formed; plants usually have the primary root and sprout but not seed lobes
Immature (*im*)	Indicators and properties that are transitional between juvenile and adult plants; branching typical of a certain species occurs; the sprouting type changes, but individual elements of the primary sprout are retained
Virginal (*v*)	Features typical of the life form of the species are formed at this stage; the plants have the adult leaves, sprouts, and root system typical of the species but do not possess generative organs
Young generative (g_1)	Characterized by the emergence of generative organs; new-growth processes prevail over die-off processes; all of the adult structures have already been formed
Middle-aged generative (g_2)	New-growth and die-off processes are in equilibrium; plants are characterized by the maximum size, the maximum number of generative organs, and the maximum annual biomass production
Old generative (g_3)	Die-off processes start to prevail; the generative function decreases; root and shoot formation is reduced
Senile (*s*)	Dead plant parts accumulate; the life form is simplified, and juvenile features emerge

Table 3
Basal area (BA) and density (D) of the tree species on the 10.5-ha sample plot.

Species	BA (m^2/ha)		BA (%)		D (stems/ha)		D (%)	
	Live	Dead	Live	Dead	Live	Dead	Live	Dead
Canopy species								
Tilia amurensis	14.31	0.00	26.5	2.7	95.8	2.0	10.6	1.9
Pinus koraiensis	11.28	0.02	20.9	11.9	49.8	4.5	5.5	4.2
Picea jezoensis	8.65	0.05	16.0	30.5	156.5	35.0	17.3	32.7
Betula costata	7.55	0.00	14.0	1.8	33.8	1.4	3.7	1.3
Ulmus laciniata	1.29	0.00	2.4	0.1	13.8	0.4	1.5	0.4
Fraxinus manshurica	0.10	0.00	0.2	0.0	1.8	0.2	0.2	0.2
Quercus mongolica	0.00	0.00	0.0	0.0	0.1	0.0	0.0	0.0
Subcanopy species								
Abies nephrolepis	7.23	0.08	13.4	51.0	323.4	52.4	35.8	49.0
Acer ukurunduense	1.77	0.00	3.3	1.7	131.5	5.7	14.6	5.3
Acer mono	1.18	0.00	2.2	0.1	37.4	0.9	4.1	0.8
Acer tegmentosum	0.20	0.00	0.4	0.1	11.6	1.0	1.3	1.0
Cerasus maximowiczii	0.14	0.00	0.3	0.1	11.4	2.3	1.3	2.1
Acer barbinerve	0.11	0.00	0.2	0.0	32.5	1.1	3.6	1.1
Taxus cuspidata	0.09	0.00	0.2	0.0	0.3	0.0	0.0	0.0
Prunus maakii	0.06	0.00	0.1	0.0	0.4	0.0	0.0	0.0
Sorbus amurensis	0.03	0.00	0.0	0.0	1.0	0.1	0.1	0.1
Syringa amurensis	0.01	0.00	0.0	0.0	2.0	0.0	0.2	0.0
Rhamnus davurica	0.01	0.00	0.0	0.0	0.1	0.0	0.0	0.0
Total	54.04	0.16	100.0	100.0	903.2	107.0	100.0	100.0

systems) or their aggregation is caused by environment heterogeneity (if they are far apart).

An important factor affecting the structure of plant patterns is the light condition mosaic determined by canopy gaps because light conditions are very important at every stage of a plant's development. Therefore, it is necessary to understand how the gaps appear during the development of plant patterns (evenly or in groups, contemporaneously or gradually) within the scope of the study territory. Gap position should correlate to the position of stumps. These stumps persist for several decades (especially coniferous stumps) (Petrillo et al., 2016). Thus, having analyzed the stump pattern structure, we can draw conclusions regarding the positions of gaps appearing over previous decades. This, together with the reconstructed disturbance history (Omelko et al., 2016), allows a characterization of the process of the appearance of gaps.

The light demands of plants increase during their development (Evstigneev, 1996). Thus, to evaluate how light condition mosaic affects plants patterns in different stages of plant development, it is also necessary to characterize increases in light demand and, accordingly, changes in plant shade tolerance.

In the light of these considerations, we set the following aims for this work: (a) to describe the evolution of spatial pattern of the dominant tree species, from early juveniles to mature, generative individuals, (b) to analyze the influence of the ontogenetic changes in shade-tolerance on pattern formation, and (c) to understand how species' life strategy traits influence pattern structure.

2. Materials and methods

2.1. Study area

The study was performed on the western macroslope of the southern part of the Sikhote-Alin mountain range (Southeastern Russia) at the Verkhneussuriysky Research Station of the Federal Scientific Center of the East Asia Terrestrial Biodiversity Far East Branch of the Russian Academy of Sciences (4400 ha; N 44°01′35.3″, E 134°12′59.8″, Fig. 1). This territory is characterized by a monsoon climate with relatively long, cold winters and warm, rainy summers. The average annual precipitation is 832 mm, and the average annual air temperature is 0.9 °C. The coldest month is January (the average temperature is −32 °C), and the warmest month is July (the average temperature is 27 °C) (Kozhevnikova, 2009). The relief is characterized by mountain slopes with angles averaging ~20°. The study area is characterized by brown mountain forest soils (Ivanov, 1964).

Mixed forests with Korean pines (Korean pine-broadleaved forests of the central type (Kolesnikov, 1956), which form an altitudinal belt up to 800 m above sea level), predominate in the study territory. At high altitudes, they are gradually replaced by coniferous fir-spruce forests (Kolesnikov, 1956). Up to 30 tree species form stands of Korean pine-broadleaved forests, which are dominated by *Abies nephrolepis* (Trautv.) Maxim., *Betula costata* (Trautv.) Regel., *Picea jezoensis* (Siebold et Zucc.) Carr., *Pinus koraiensis* Siebold et Zucc. and *Tilia amurensis* Rupr (Kolesnikov, 1956). The characteristics of these dominant species are provided in Table 1.

Our study is based on data collected in two permanent sample plots of 1.5 ha (150 × 100 m) (Omelko and Ukhvatkina, 2012) and 10.5 ha (300 × 350 m). The first plot is located in the middle of the west-facing slope that has an angle of 22° and an altitude 750–950 m above sea level. The second plot is situated in the upper and middle portions of the west, south-west and north-west-facing slopes at an angle of 10–25°. The distance between the two plots is approximately 200 m, and both were set up in a late-successional stand of the middle type of Korean pine-broadleaved forests at the upper boundary of the distribution of Korean pine, where it forms mixed stands of Korean pine-spruce and spruce-broadleaved forests (Kolesnikov, 1956).

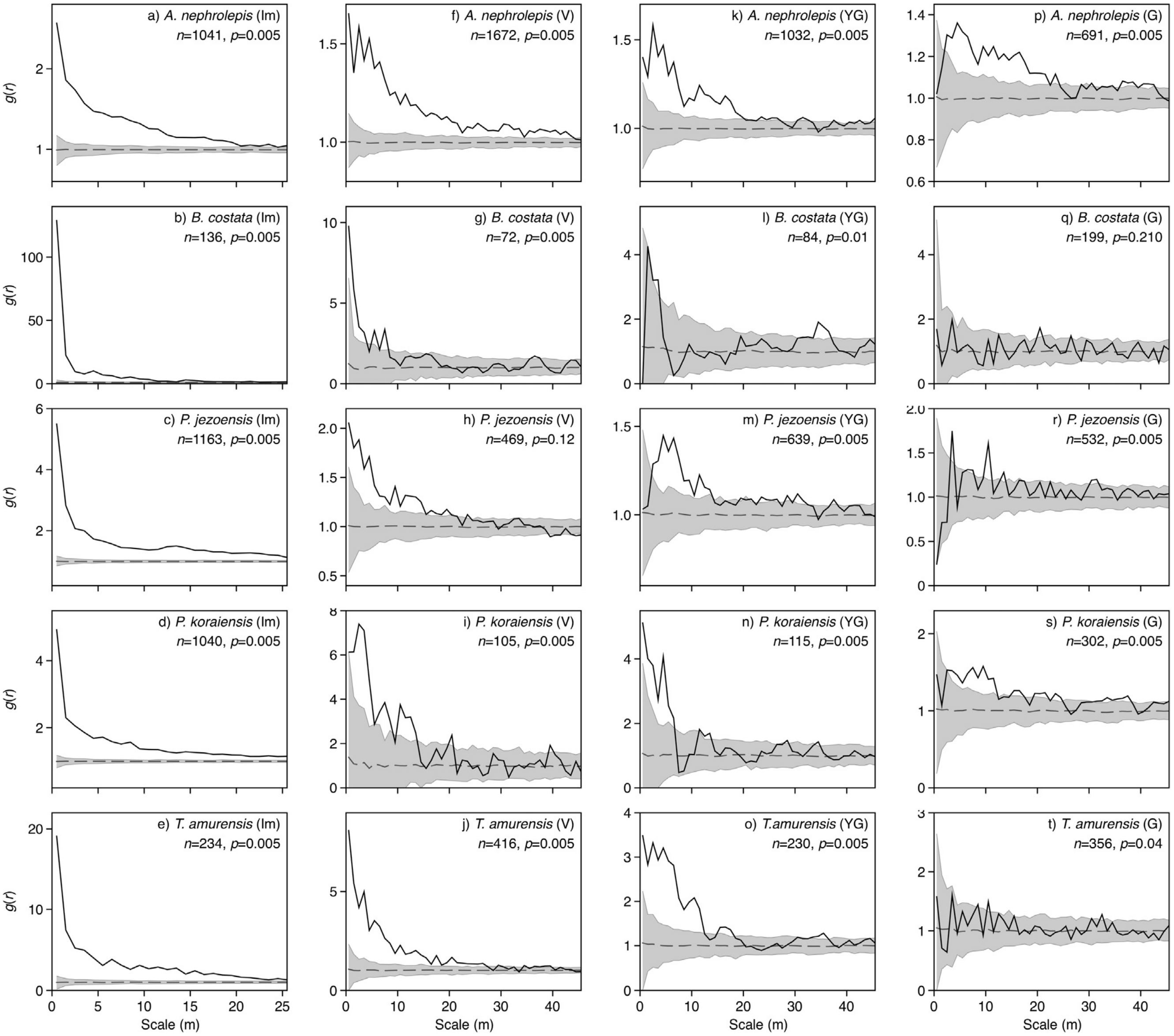

Fig. 2. Univariate point pattern analyses of five dominant species using pair-correlation function. The insets show the analyses of point patterns of different ontogeny stages: Im - immature plants (im_1, im_2, im_3), V - virginal plants (v_1, v_2), YG – young generative plants (v_2, g_1), G – middle- and old-generative plants (g_1, g_2). Solid line indicates the empirical curve, dashed line indicates the expected value under the null-model CSR, gray area indicates limits of 99% simulation envelope; n is number of plants and p is p-value of the GoF test.

In addition to the five dominant species referred to above, the stands in the plots included the following tree species: *Acer barbinerve* Maxim., *Acer mono* Maxim., *Acer tegmentosum* Maxim., *Acer ukurunduense* Trautv. et Mey., *Fraxinus mandshurica* Rupr., *Cerasus maximowichzii* (Rupr.) Kom., *Sorbus amurensis* Koehne, *Prunus maakii* Rupr., *Quercus mongolica* Fisch ex Ledeb., *Rhamnus davurica* Pall., *Syringa amurensis* Rupr., *Taxus cuspidata* Siebold et Zucc. ex Endl., and *Ulmus laciniata* (Trautv.) Mayr. There were also the scrubs *Eleutherococcus senticosus* (Rupr. & Maxim.) Maxim., *Philadelphus tenuifolius* Rupr. et Maxim., *Ribes maximoviczianum* Kom. and the lianas: *Actinidia kolomikta* Maxim. et Rupr., and *Schizandra chinensis* (Turcz.) Baill.

2.2. Data collection

We performed a census of the plots during the field seasons of 2010–2015. Both plots were divided into 10 × 10 m square areas, and the surveys were conducted within those squares. All living trees were stem-mapped, tagged, and identified to the species level. The ontogenetic stage (Table 2; Appendix A, Table A1) of *A. nephrolepis*, *P. jezoensis* and *P. koraiensis* were determined based on studies of their ontogenesis (Komarova and Trofimova, 2010; Komarova et al., 2010; Ukhvatkina et al., 2010). For the remaining tree species, we referenced the general signs (Smirnova and Bobrovskii, 2001; Evstigneev and Korotkov, 2016). In the 1.5-ha sample plot, we considered living plants at the following ontogenetic stages: immature (3 phases), virginal (3 phases), and generative (young generative, middle-aged generative, and old generative). In the 10.5-ha sample plot, we used the same classification but discarded the immature stage. In addition to the living trees, we also stem-mapped the dead trees and recorded their before-dying ontogenetic stage. To determine the approximate locations of the canopy gaps that were formed in the last decades, we also stem-mapped the stumps in the 10.5-ha area (the before-stump ontogenetic stage and the species were also stated). To characterize the gaps (number and size distribution), we measured all the gaps on a 6-ha part of the 10.5-ha sample plot.

In the 1.5-ha sample plot, we estimated the tree crown mean radii at different ontogenetic stages. For this we measured their radii in four directions from the tree trunks (north, south, east, and west).

To characterize increased light demand during plant development,

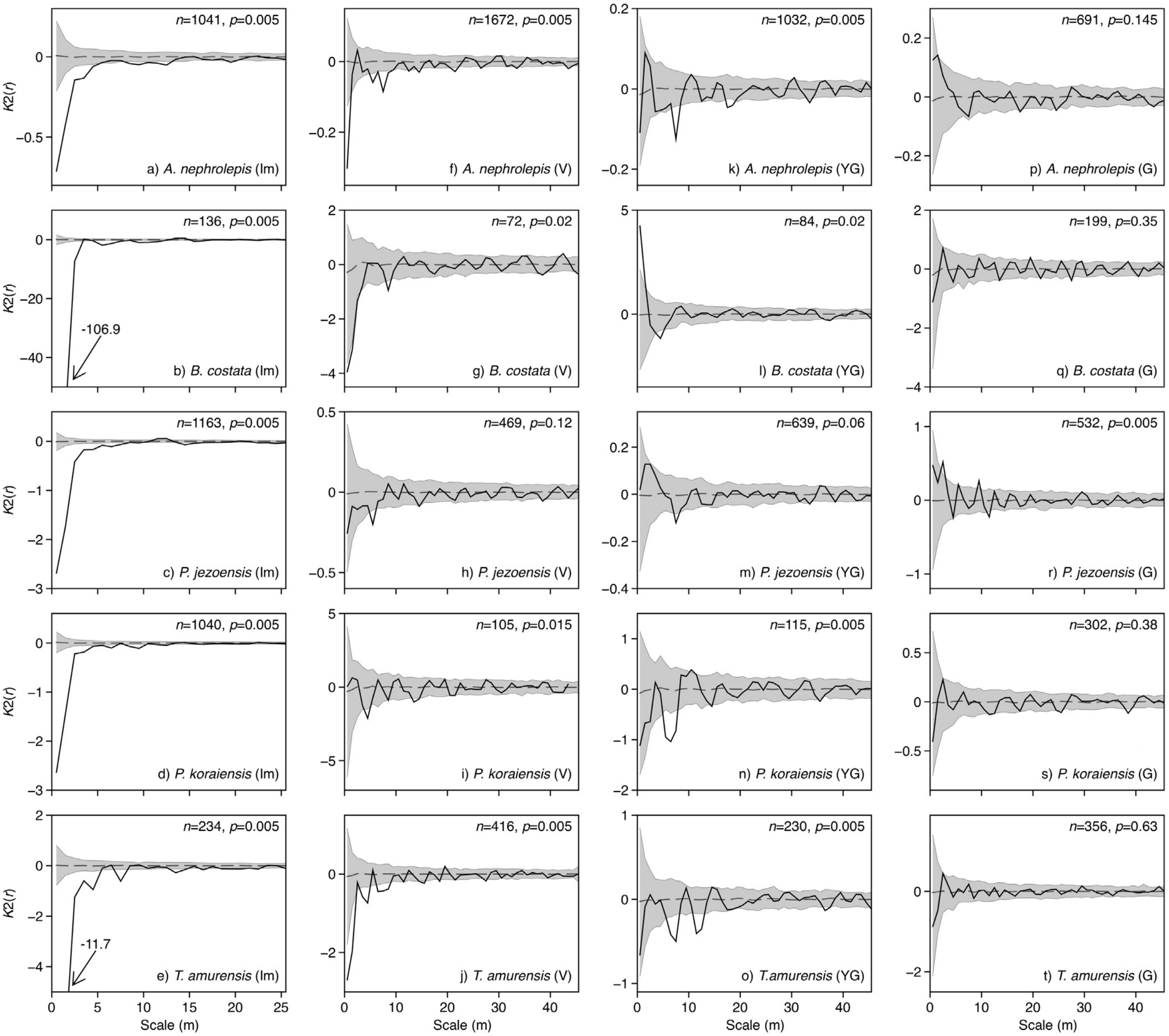

Fig. 3. Univariate point pattern analyses of five dominant species using $K2(r)$ function. The insets show the analyses of point patterns of different ontogeny stages: Im - immature plants (im_1, im_2, im_3), V - virginal plants (v_1, v_2), YG – young generative plants (v_2, g_1), G - middle- and old-generative plants (g_1, g_2). Solid line indicates the empirical curve, dashed line indicates the expected value under the null-model CSR, gray area indicates limits of 99% simulation envelope; *n* is number of plants and *p* is *p*-value of the GoF test.

we stated the vitality of the immature, virginal and young generative plants (Appendix A, Table A2). For these plants, we assigned also the gap positions based on plants being under, on the periphery of or outside the crowns of canopy species. We used three categories: (1) in the gap, (2) on the periphery of the gap, and (3) under the canopy. Plants whose crowns were situated within the gap boundaries were placed in the first category. Plants whose tops were situated either at gap boundaries or under the stand canopy or that had parts of their crowns under the stand canopy where placed in the second category. We also placed deciduous plants into that category if their bases were under the canopy but their crowns were partially or totally stretched into the gaps (as deciduous plants are more flexible than coniferous plants). Plants whose crowns were completely covered by canopy were placed into the third category. To test the independence of stage, vitality, canopy position and species an analysis of contingency tables was performed using chi-square tests in R (R Core Team, 2017).

2.3. Radiocarbon dating of soil charcoal

To date fire disturbances in the stand, we performed a search and collection of soil charcoal for radiocarbon analysis (^{14}C). The search for samples was performed in the mounds of uprooted trees in the territory of the sample plots. The specimens were prepared and dated at the CCU Laboratory of Radiocarbon Dating and Electron Microscopy of the Institute of Geography RAS and at the Center of Applied Isotope Studies (University of Georgia, USA). The results were calibrated using the radiocarbon calibration program CALIB rev7.1.0 (Copyright 1986-2016 M Stuiver and PJ Reimer).

2.4. Point pattern analysis

For "real-world" patterns, which often show aspects of heterogeneity, it is especially important to use several summary statistics of different natures to describe various aspects of pattern structure (Illian et al., 2008; Wiegand et al., 2013). We used the following summary

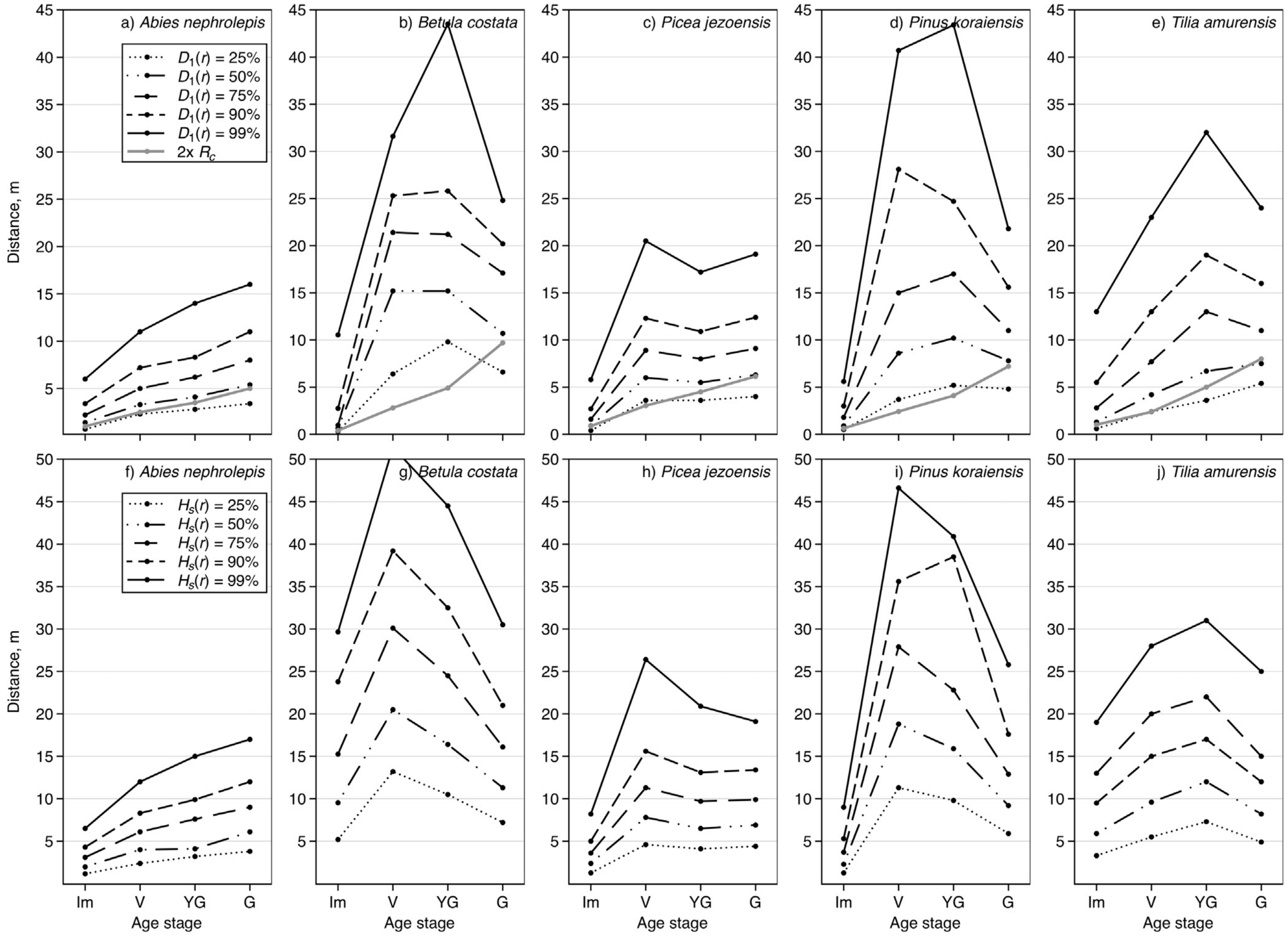

Fig. 4. Distribution of distances from focal plant to its first nearest neighbor plant $D_1(r)$ (a–e) and sizes of the empty areas without points in the plants patterns $H_s(r)$ (f–j) of five dominant species in different ontogenetic stages. 2× R_c is twice the average crown radii (maximum distance at which crowns of plant pairs can interact with each other).

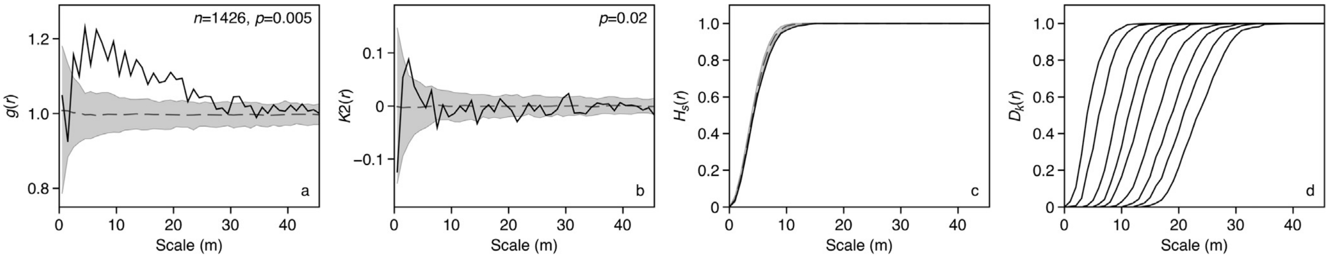

Fig. 5. Univariate point pattern analyses of stumps using four summary statistics: (a) pair-correlation function, (b) $K2$-function, (c) spherical contact distribution function H_s, and (d) distance to kth neighbor D_k. Solid line indicates the empirical curve, dashed line indicates the expected value under the null-model CSR, gray area indicates limits of 99% simulation envelope.

statistics in this study: (a) pair-correlation function $g(r)$ (Stoyan and Stoyan, 1994), (b) $K2$ function (Schiffers et al., 2008), (c) distance distribution to the kth neighbor $D_k(r)$ (Diggle, 2003; Illian et al., 2008), and (d) spherical contact distribution function $H_s(r)$ (Diggle, 2003; Illian et al., 2008).

Because the plant patterns we analyzed in this study (especially immature and virginal) were heterogeneous, which became obvious at the data collection and pattern visualization steps (see Appendix A, Figs. A1–A5), we used the $K2(r)$ function in this work to account for virtual aggregation. The $K2(r)$ function shows the expected differences in point number between consecutive distances. It can be heuristically interpreted as the first derivative of the $g(r)$ function (Schiffers et al., 2008):

$$K2(r) = dg(r)/dr.$$

A positive value indicates a transition from low to high intensity and consequently, the upper limit of the range of scales at which the pattern has a regular structure. A negative value shows a transition from high to low intensity and consequently the upper limit of the scale range at which the pattern is aggregated.

The cumulative distribution function $D_k(r)$ of the distances r to the kth neighbor presents the probability that the typical point of a pattern has k neighboring points within radius r. The values of functions range from 0 (distance at which neighboring points of the pattern are absent) to 1 (distances from which all points of the pattern have the kth nearest neighbor).

The spherical contact distribution function $H_s(r)$ is closely related to the distribution function of distances to the nearest neighbor $D_k(r)$.

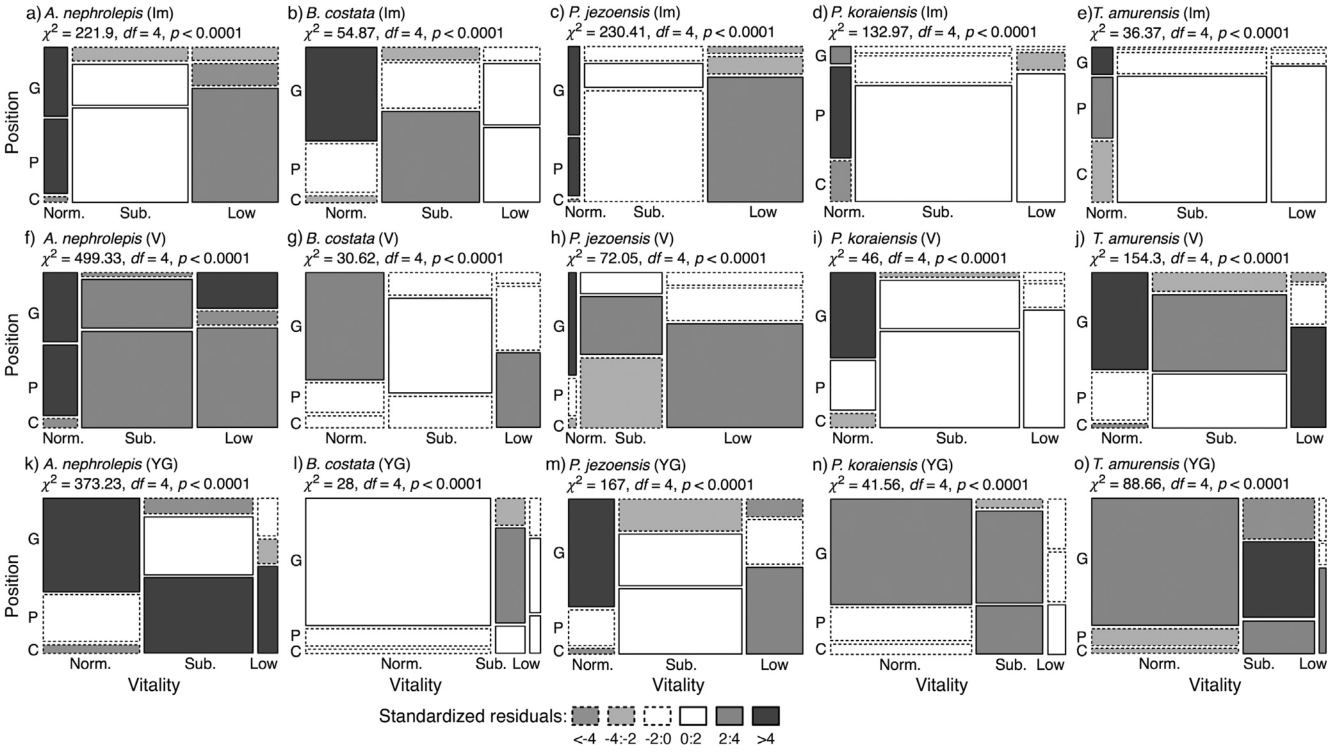

Fig. 6. Mosaic plots of the observed frequency of normal, subnormal and low vitality plants in different positions relative canopy and gaps: Im - immature plants (im_1, im_2, im_3), V - virginal plants (v_1, v_2), YG – young generative plants (v_2, g_1). Positions: G denotes "gap", P denotes "gap periphery" and C denotes "canopy". The area of each rectangle is proportional to the cell frequency of the corresponding contingency table. Solid and broken lines indicate positive and negative deviations from expected frequencies, respectively. The shading of each rectangle is proportional to standardized residuals from the fitted model (values indicated in the legend). Light gray and black rectangles indicate significant deviations from the expected cell frequencies (at ca. $\alpha = 0.005$, $\alpha = 0.0001$, respectively).

Unlike the $D_k(r)$ function, which shows the distance between two points, the $H_s(r)$ function shows the distribution of distances from a "random" test location to the nearest pattern point. As well as $D_k(r)$, the $H_s(r)$ function is a cumulative function with values from 0 to 1. The $H_s(r)$ function is used to characterize nonstationary patterns with extensive empty areas without points, i.e., it measures the "gap" size distribution in the pattern.

For the analysis, plants from separate ontogenetic stages were united into age groups: (a) immature plants (im_1, im_2, and im_3), (b) virginal plants (v_1 and v_2), (c) young generative plants (v_3 and g_1), and (d) middle- and old-generative plants (g_2 and g_3). This is because plants at some stages, particularly v_3 and g_1, were too rare for analysis (50–70 plants were required) (Wiegand and Moloney, 2014). The virginal plants of the third subgroup were united with the first generative subgroup, as they are in the transitory state, which depends not on their physiological development, but on environmental conditions (Smirnova and Bobrovskii, 2001).

The analysis was performed using the Programita software package (Wiegand and Moloney, 2014). To describe the pattern structure formed by plants of different ontogenetic stages, we used a univariate analysis with null model CSR (complete spatial randomness). The data from the 1.5-ha sample plot were used to describe the immature plants' patterns structure, and for the other ontogenetic stages and the stumps, we used data from the 10.5-ha sample plot. For immature plants, the grid was 1 × 1 m, and the maximal distance of analysis was 25 m. For virginal, young generative, middle- and old-generative plants and stumps, the grid was 3 × 3 m, and the maximal distance of analysis was 45 m. To analyze stump pattern structure, we used data from the 10.5-ha sample plot (stumps of middle- and old-generative trees, as their downfalls formed the gaps) with the null model CSR; the grid was 3 × 3 m. In all analyses, we used the four summary statistics indicated above. Employing $D_k(r)$, we found the detection probabilities of the 1st, 2nd, 4th, 6th, 8th, 12th, 16th, 20th and 25th neighboring plants. Additionally, in order to determine whether aggregation of plants changes in different ontogenetic stages, we tested the $g_{11}(r)$-$g_{22}(r)$ statistic (difference of $g(r)$ functions for immature and virginal, virginal and young generative, young generative and middle- and old-generative plants) against the "independent marking" null model. A significant departure was noted from the null model we evaluated using the fifth lowest and highest values of 199 Monte Carlo simulations of the null model to generate approximately 99% simulation envelopes (Wiegand and Moloney, 2014). We also used a goodness-of-fit (GoF) test to assess significant departures from the null model.

3. Results

3.1. Stand structure and ages of fire disturbances

In the 1.5-ha sample plot, there were 6479 living trees and 195 dead trees. In the 10.5-ha sample plot, there were 9571 living trees and 1143 dead trees. The stand on the 10.5-ha sample plot was formed of 18 tree species (Table 3). In terms of basal area, *T. amurensis* prevailed among the trees forming the stand canopy and was followed by *P. koraiensis*, *P. jezoensis* and *B. costata*. The overall portion of the remaining canopy tree species was 2.6%. The prevailing subcanopy species was *A. nephrolepis*, followed by *A. ukurunduense* and *A. mono*. The portion of the remaining eight species was rather small—1.2% overall. *P. jezoensis* prevailed for the number of trees in the canopy, and there were slightly fewer trees of *T. amurensis*. Among the subcanopy species, the number of *A. nephrolepis* was maximal. A comparison of the basal areas and tree densities showed that *P. koraiensis* and *B. costata* were represented by relatively less abundant large trees, whereas *T. amurensis*, *P. jezoensis* and *A. nephrolepis* were represented by more abundant but smaller trees.

Thus, the basal area of the five dominant species was 90.8% of the total; four of which were related to the canopy (*T. amurensis*, *P.*

jezoensis, *P. koraiensis, B. costata*) and the last to the subcanopy (*A. nephrolepis*). *P. jezoensis* and *A. nephrolepis* prevailed among deadwood; their basal area was 81.5% of total, and their density and basal area ratio was the same as for living trees.

The 1.5-ha plot characteristics were rather similar, including the list of dominant species, their rank by basal area and stem density, and the overall portion of their total basal area (Omelko et al., 2016). The difference was that in the 10.5-ha sample plot, the basal area for *T. amurensis*, *P. koraiensis* and *B. costata* was larger. In addition, based on the ratio between the basal area and stems density, we can conclude that on the 10.5-ha sample plot, trees of *T. amurensis* and *P. koraiensis* had, on average, larger diameters.

The percentage of gaps in the canopy of the stand was 30.2% of the total area. The number of gaps per hectare was 43.3. Slightly more than half (51%) of the gaps had areas up to 25 m^2, and gaps with areas of 25 to 100 m^2 made up an additional 28.5% (Appendix A, Fig. A9). Gaps with sizes greater than 250 m^2 were rare (4.6%), and the average gap size was 69.6 m^2.

Charcoals were found in two mounds after treefalls in the study area. According to the radiocarbon dating results, their ages were close: 1955 ± 20 BP ($IGAN_{AMS}$5637) and 2090 ± 25 BP ($IGAN_{AMS}$5282). This suggests that the last fire in this area occurred at approximately 2000 BP. We also found no fire scars on the core samples, cross-cut samples, or living trees.

3.2. Plant patterns structure at different ontogenetic stages

3.2.1. Immature plants

The empirical curves of the pair-correlation functions for all five species were situated above the upper simulation interval throughout the entire distance of analysis and became approximately parallel to the abscissa axis, which can be interpreted as “virtual aggregation” (Wiegand and Moloney, 2014) (Fig. 2a–e). The $K2(r)$ function revealed plant aggregated distributions at several spatial scales: all five species had clusters with sizes (radii) of approximately 4.5–7.5 m and 11.5–14.5 m (Fig. 3a–e). In addition, we revealed clusters of *B. costata* with sizes of approximately 2.5 m. The comparison of cluster sizes with a set of functions of distributions of distances to the *k*th neighbor $D_k(r)$ showed (Appendix A, Fig. A6a–f) that for sizes between 2.5 and 7 m, the clusters were formed by 12–26 plants, and the clusters with larger sizes were formed by more than 26 plants. The distances between the neighboring plants were relatively small, for four of five species and for half of the plants, the nearest neighboring plant was within 1–1.4 m (for *B. costata* within 0.6 m) (Fig. 4a–e).

3.2.2. Virginal plants

The empirical curve characterizing the *A. nephrolepis* pattern was situated above the upper simulation interval for the entire distance of analysis (“virtual aggregation”) (Fig. 2f). For other species, the pair-correlation function revealed an aggregated distribution: clusters with average sizes of approximately 8.5 and 12.5 m (*B. costata* and *P. koraiensis*) and approximately 20.5 m (*P. jezoensis* and *T. amurensis*) (Fig. 2g–j). The $K2$ function revealed the aggregated distribution at several spatial scales (Fig. 3f–j). For three species (*A. nephrolepis*, *B. costata* and *T. amurensis*), small clusters with average sizes of 0.5–2.5 m were revealed.

For four of five species (except *P. jezoensis*), clusters with average sizes of approximately 5.5–10.5 m were revealed. Clusters with sizes from 0.5 to 10.5 m were formed by two or three plants (5–7 for *T. amurensis* and 9 for *A. nephrolepis*). The distances between the neighboring plants, and compared to immature plats, were enlarged up to 2.5-fold (*A. nephrolepis*) and 23-fold (*B. costata*). The distances from the single plants to their nearest neighbors were enlarged 2- to 7-fold (Fig. 4a–e).

3.2.3. Young generative plants

The pair-correlation function revealed an aggregated distribution of all five species (Fig. 2k–o); for *A. nephrolepis*, the average cluster sizes were approximately 20.5 m (*B. costata* – 2.5 and 34.5–36.5 m, *P. jezoensis* – approximately 13.5 m, *P. koraiensis* – 6.5 m, and *T. amurensis* – 18.5 m). The $K2(r)$ function revealed plant aggregations at 1–2 spatial scales (Fig. 3k–o). Clusters with sizes of 0.5–2.5 m, which were present at the previous generative stage, “disappeared”. For four of five species (except *P. jezoensis*), clusters with sizes of approximately 6.5–9.5 m were revealed. For *P. jezoensis*, there was a tendency for cluster formation with those sizes. Regarding *T. amurensis*, clusters were revealed with sizes of 13.5 m. Clusters sized 6.5–9.5 m were formed by two or three plants. Compared to the virginal stage, the distances between the neighboring plants were approximately identical (*B. costata* and *P. jezoensis*) or for other species were 1.2- to 1.5-fold larger (Fig. 4a–e).

3.2.4. Middle- and old-generative plants

The pair correlation functions for one species of the five (*B. costata*) showed random plant distributions (Fig. 2q and t). Aggregated distributions were revealed for *A. nephrolepis* (average cluster sizes of 24.5 m and 34.5–41.5 m), *P. jezoensis* (average cluster sizes of approximately 4.5–11.5 m), *P. koraiensis* (cluster sizes from 13.5 to 37.5 m), and *T. amurensis* (average cluster sizes of 10.5–15.5 m and 30.5–34.5 m) (Fig. 2p, r, s, and t). The $K2(r)$ function showed the random plant distributions for four of five species (except *P. jezoensis*) (Fig. 3p–t). We should note the formation of aggregates of *P. jezoensis* (sizes of approximately 12 m for 5 plants). The change in distance between neighboring plants compared to young generative plants was differently directed. For *P. koraiensis*, it increased 1.3-fold, and for other species, it decreased 1.1- to 1.3-fold. In addition to the enlarged distance (1.1-fold) between the single plants to their nearest neighbors for *A. nephrolepis* and *P. jezoensis*, for other species, it decreased 1.3- to 2-fold.

Comparisons of the pair correlation functions for different ontogenetic stages showed (Appendix A, Fig. A9) that the immature plants of four of the five species were more aggregated than virginal plants at scales of 1–2 m. Virginal plants were more aggregated at a scale of 2–4 m only for *P. koraiensis*. Virginal plants of *P. jezoensis*, *P. koraiensis* and *T. amurensis* were more aggregated than young generative plants at scales up to 5–10 m. The aggregations of middle- and old-generative plants for three species differed from those of young generative plants: *B. costata* and *T amurensis* generative plants were less aggregated on scales of 2 m and 1–11 m, respectively, and *P. koraiensis* plants were more aggregated at a scale of 5 m.

3.3. Stumps pattern structure

The analysis of stump pattern structure using the pair-correlation function revealed aggregates with an average radius of approximately 27.5 m (Fig. 5a). The $K2(r)$ function showed a rather random distribution (Fig. 5b). This suggests the existence of large patches of randomly located stumps, with more than 25 stumps in each patch (Fig. 5d). A visual inspection of the stump mosaic also confirms this. The empty area distribution (areas without stumps) was nearly expected given their random distribution (Fig. 5c).

3.4. Plant vitality depends on position relative to canopy and gaps

There were significant differences in the frequencies of plants of different vitalities depending on position relative to the canopy and gaps for all ontogenetic stages (Fig. 6). At the immature stage, plants situated under the canopy prevailed (Fig. 6a–e). There were 1.5 (*B. costata*) to 44 (*T. amurensis*) times more plants under the canopy than in the gaps. However, almost all (95–100%) had low vitality. Thus, for all the species, the frequencies of plants of normal vitality were significantly higher than expected in the gaps and on their peripheries.

Under canopy, the frequency of plants of low vitality was higher.

At the virginal ontogenetic stages of *B. costata* and *T. amurensis*, the distribution of the numbers of plants changed; the plants at the gap peripheries prevailed, and the number of plants under canopy decreased (Fig. 6g and j). For coniferous species, the distributions of the numbers of trees remained almost the same, with maxima under the stand canopy (Fig. 6f, h, and i). However, again for all five species, the frequencies of plants with normal vitality were significantly higher than expected at the gap peripheries or in the gaps.

Finally, at the young generative stage, for four of five species (except *P. jezoensis*), plants in the gaps prevailed (Fig. 6k–o). For *B. costata, T. amurensis*, and *P. koraiensis*, the total numbers of plants under the canopy considerably decreased (20-, 3- and 6-fold, respectively, compared to the number of plants in the gaps). There were almost no plants of low vitality in the gaps (the frequencies were significantly lower than expected). For four of five species (except *P. jezoensis*), plants of normal vitality prevailed, and for all species, their frequencies were significantly higher in gaps. The proportion of plants of low vitality decreased up to 50–78% for *B. costata*, *P. koraiensis* and *T. amurensis*, but for *A. nephrolepis* and *P. jezoensis*, it remained high at 92% and 98%, respectively. Their frequencies were significantly higher than expected under canopy or at the peripheries of gaps.

4. Discussion

4.1. Plants pattern formation process and the influence of shade-tolerance

The results of radiocarbon dating showed that the last fire on the territory of the investigated stand occurred approximately 2000 years ago. For the formation of a natural structure of an old-growth stand after a severe disturbance (including fire), at least three generations of trees of the longest-lived key species are needed (East-European Forests (Russia), 2004), giving the lifetime of *P. koraiensis* (Table 1) for the stand at this time of approximately 1500 years. Therefore, we can confirm that the structure of the stands in the plots was not affected by severe fire, the main disturbance factor in these forests.

The transformations of plant pattern structure for the various species at different stages of ontogenetic development had common features. For all five species, it proceeded from a pronounced aggregated distribution at the immature stage to a random distribution in the middle- and old-generative stages. Second, at the middle- and old-generative stages, the patterns of all species were more homogeneous, and at the transition from immature to virginal stage, the distances between the neighboring plants and empty areas without plants was enlarged but then lessened in the middle- and old-generative stage. Third, the cluster sizes formed with the plants at the immature, virginal and young-generative stages were similar. In most cases, the cluster sizes were 4.5–8.5 m (approximately 40% of the cases) and 12.5–16.5 m (approximately 30% of the cases). Comparison of the distribution of the distances to the nearest neighbor $D_1(r)$ and twice the average radius of crowns (Fig. 4a–e) shows that at the immature ontogenetic stage approximately 35% of trees could interact with the crown or root systems (we assumed that root system size is approximately equal to crown size (Karpov, 1969)). In the virginal and young generative ontogenetic stage that proportion decreased to 10–35%. Therefore, we can conclude that the revealed clusters were not conditional on plant interaction, as they were located far from each other, but were influenced by other factors.

Decreases in aggregation with plant development have been reported in many other studies (e.g., Kenkel, 1988; Harms et al., 2001; Hao et al., 2007; Zhang et al., 2010a, 2010b; Liu et al., 2014). The evolution of the spatial pattern of trees in different developmental stages is due to the self-thinning process (Piao et al., 2013) and environmental changes in the forest community (Harms et al., 2001). With increasing size of trees, intra- and interspecific competition increases, causing self-thinning. The patterns of generative plants were random, but not regular, as the results of some other studies have shown (e.g., Kenkel, 1988). We believe that one of the reasons is that the stand is formed by coniferous species that have conical and ovoid shaped crowns, and deciduous species that have back-ovate or umbellate shaped crowns (Usenko, 1968, Komarova et al., 2010; Komarova and Trofimova, 2010; Ukhvatkina et al., 2010). In addition, the shade tolerance of conifers is generally higher than that of deciduous species (Usenko, 1968). This allows the crowns of deciduous and coniferous species to overlap slightly, and therefore competition between plants is less intense.

The patterns of the studied stand are transformed in this way and can be explained in more detail using results from this and previous work. The immature plants of different species can accumulate under the stand canopy (Ukhvatkina et al., 2011). Most of these plants were under the stand canopy, so they had developed slowly and had low vitality (suppressed plants) (Fig. 6a–e). After gap formation, they could increase in height dramatically and advance to the virginal and the young generative stages (Ukhvatkina et al., 2011, 2015). At these stages plants of all species, both coniferous (usually recognized to be shade-tolerant) and deciduous (considered to be light-requiring) require abundant light for development, which they can obtain by growing only in the gaps or at their peripheries. This follows from the change in the distribution of the number of normal-vitality plants (Fig. 6f–o). In addition, this stand is characterized by a low- and medium-intensity disturbances regime (Ukhvatkina et al., 2015; Omelko et al. 2016). From time to time, only single gaps appear in the stand as a result of tree downfall, or groups of gaps or when neighboring trees die. Over a period of decades, the gaps had become randomly distributed, which was evidenced in the random disposition of stumps from dead trees (Fig. 5b). Thus, the process of gap formation in the stand canopy is rather stochastic.

By comparing these results, we can make the following conclusion—although all five dominant species accumulate and form aggregations at the immature stage, for further development at the virginal and young-generative stages, they must be in gaps. However, these gaps form rarely, and their locations in the territory are random. That is why the transition to the virginal stage becomes a bottleneck for the plants. This is also indicated by ontogenetic spectra, which are bimodal, having two population peaks of immature and middle-generative plants (Omelko et al., 2016) and relatively low numbers of virginal plants. Thus, regardless of the characteristics of the immature plant aggregations, their pattern goes through “the filter” of randomly located gaps in the stand canopy. After such “filtering,” the dense clusters of immature plants (more than 26 plants with cluster sizes of 11.5–14.5 m) remain far less denser clusters of virginal plants (2–3 plants for *B. costata*, *P. jezoensis*, *P. koraiensis* and 5–9 plants for *A. neprolepis* and *T. amurensis*, with cluster sizes of 0.5–10.5 m), and clusters of 2–3 young-generative plants with sizes 6.5–9.5 m. Decrease in the size of clusters is most likely due to the fact that the average size of gaps (in accordance with their area of 69 m^2) is smaller than the sizes of clusters of immature and virginal plants. A comparison of the pair correlation functions for different ontogenetic states $g_{11}(r)$-$g_{22}(r)$ shows (Appendix A, Fig. A9) that in most species, the aggregation between the immature and virginal stage, the virginal and young generative stage and the young generative and generative stage decreases. At the middle- and old-generative stages, the clusters finally disappear. The decrease in the density of plants and the disappearance of the aggregated pattern throughout ontogeny is probably the result of strong competition in the gaps (Kenkel, 1988; Piao et al., 2013). Plants that reach this stage stay there for a long time, i.e., half or even more of their lifetimes (Omelko et al., 2016). As a result, they accumulate at this stage (except *A. neprolepis*), and their pattern compared to that of the previous ontogenetic stage becomes more homogeneous.

The details of the processes of pattern formation of different species of immature plants and their further transformation in the course of plant ontogenetic development differ somewhat, which could be explained by the features of their life strategies. These include shade-tolerance at different ontogenetic stages, namely, how much light is needed for development and how long they can exist under suppression.

Because immature coniferous plants are relatively more shade-tolerant than deciduous plants (Usenko, 1968), they extend everywhere throughout the plot and form large clusters at different spatial scales. Such clusters can arise because conifer plants recruit in gaps, and after a gap is closed, they can be under suppression for some decades (the maximal immature plant age is indicative of this). Therefore, they could accumulate successively in clusters at different spatial scales. However, *B. costata* plants were distributed on the plot in isolated, relatively dense clusters (Fig. 3b and e), and that, in addition to its smaller maximal age, shows that they are more dependent on the gaps at present. *T. amurensis*, judging by the structure of its pattern and location of plants relative to the canopy gaps, has a higher shade tolerance than that of *B. costata*. Therefore, its plants form clusters of larger sizes and occupy a relatively large part of the sample plot.

At the virginal and young-generative stages, the plants of *A. nephrolepis* and *P. jezoensis* are characterized by high shade-tolerance, as demonstrated by the fact that many plants of these species are situated under the stand canopy (Fig. 6f, h, k, and m). That is why the pair-correlation function revealed aggregation on a large scale (up to 20.5–22.5 m) (Fig. 2f, k, h, and m), and the $K2(r)$ function showed a random distribution for *P. jezoensis* and clusters of smaller average radius (0.5–10.5 m) for *A. nephrolepis* (Fig. 3f, k, h, and m). The plants of *B. costata* must be in the gaps at the virginal stage; even at that stage, only single plants and small clusters formed by two plants remain. As well, there are few plants of *P. koraiensis* at the virginal and young generative stages, as their shade-tolerance decreases, and the plant numbers remain low under the canopy compared to other coniferous species (Fig. 6i and n). However, because it is a coniferous species, and its shade-tolerance is relatively higher than that of *B. costata*, the plants form clusters, and their sizes approximately coincide with the results of the pair-correlation function and $K2(r)$ function. Virginal and young-generative plants of *T. amurensis* increase in height rapidly (Usenko, 1968), and immature plants are not so densely disposed, as for *B. costata*. Thus, at the emergence of favorable conditions, the neighboring plants can develop relatively simultaneously and form small clusters of 2–6 plants. These clusters disappear only at the generative stage, when competition between the neighboring plants apparently increases.

4.2. Spatial pattern of the generative stage

The comparisons of the results using different summary statistics leads us to conclude that generative plant distribution is random, although a large-scale heterogeneity is revealed by the pair-correlation function. As shown above, the random distribution of middle- and old-generative plants is conditional on the filtering of plant patterns of previous ontogenetic stages by randomly formed gaps. However, we should consider that the gap formation process cannot be absolutely stochastic, as local disturbance histories can vary in different parts of the stand (Svoboda et al., 2014; Trostiuk et al., 2014). The pair-correlation function revealed a stump aggregation of scale of approximately 27.5 m (Fig. 5a), suggesting the heterogeneity of disturbances.

Thus, aggregation revealed with the pair-correlation function is most likely conditional on the local histories of stand disturbances. This helps to explain the existence of clusters with sizes of 15–20 m for *A. nephrolepis*, *P. koraiensis* and *T. amurensis* (Fig. 2p, s, and t). Clusters with larger sizes (up to 41 m) can likely be attributed to factors caused by territory topographic peculiarities (Kanagaraj et al., 2011; Shipley et al., 2012; Punchi-Manage et al., 2014; Do et al., 2015) or soil composition characteristics (Zhang et al., 2010a, 2010b; Zhang et al., 2011). Such habitat filtering appears to be more important at larger scales, at which predictable environmental and topographic gradients occur (Shipley et al., 2012).

In connection with the results obtained, an important question arises: if the distribution of generative plants is random (its intensity is unequal throughout the studied area), will every new vacated place that emerges after a tree's death be taken up by a tree of any species? The answer will depend on the time interval used. At the century scale, the answer will be "yes"; every site could be taken up by the plants of any species, and the random distribution of generative plants attests to that. However, at the decade level, the answer will be "no"; the species of the tree that will take up the gap depends on the history of the site before gap formation. In particular, immature plants of *A. nephrolepis* and especially *P. jezoensis* and *B. costata* require fallen dead trees to rise on this site, and those dead trees must be at a particular decomposition stage (Ukhvatkina et al., 2010; Komarova, 1986). Otherwise, the gap will be taken up by other species, e.g., *P. koraiensis* or *T. amurensis*. Thus, in considering each site, we can find long chains passing to the stand past. There are many possible combinations of the presence and absence of undergrowth of different species at different sites, and thus, in any case of middle- and old-generative plant death, the overgrowth of the emerged gap will occur in its own way.

The final patterns of middle- and old-growth generative plants are random and have only minor differences. This means that the different traits of life strategies balance each other out. As a result, if we analyze the pattern formation process on a century scale, we see that the plants of different species act analogously in their development. This fact suggests that no species have considerable advantages over others and therefore, it fits the predictions of the neutral theory (Hubbell, 2001).

4.3. Implications for conservation and management

Despite the relatively wide distribution of Korean pine and Korean pine-broadleaved forests in Northeast Asia, old-growth forests with Korean pine have only been preserved in northeast China and southeast Russia (Krestov, 2003). These unique forests have a complex spatial and vertical structure (Kolesnikov, 1956) and are characterized by a high level of biodiversity. In particular, within the Sikhote-Alin, there are more than 600 rare species of plants and animals, including ginseng and the Amur tiger.

Our study has shown that for dominant tree species, a random distribution of generative individuals is characteristic. The formation of such a pattern structure is due to small and medium-scale disturbances typical for the stands (Ishikawa et al., 1999; Zhang et al., 2014; Omelko et al., 2016). The random distribution of individuals causes a variety of variants with local species composition. In turn, this may contribute to environmental heterogeneity and increased species diversity (Connel, 1978). The process of formation of generative individual patterns is slow due to their lifetimes, e.g., 300–600 years for *P. koraiensis* and 120–240 years for *B. costata* (Omelko et al., 2016). This means that Korean pine-broadleaved forests are sensitive to severe disturbances because plants require long periods of time to regain their places in the community, and time is also needed for species to mix and form patterns with a random structure due to random small disturbances. Thus, our results once again show that to maintain biodiversity for these forests, it is necessary to develop a specific management regime that mimics the regime of natural disturbances (i.e., disturbances of medium and low intensity randomly distributed over the territory).

Our results also show that even for shade-tolerant species, improved light conditions are necessary for development in the virginal and young generative ontogenetic stages. This is important, as is tradition for the restoration of the Korean pine-broadleaved forests when shade-tolerant species such as Korean pine are planted under the closed canopies of deciduous species. It is assumed that they are sufficiently shade-tolerant to develop in such environments. However, for their successful growth, it is necessary, for example, to create artificial gaps in the canopies of deciduous species.

Acknowledgments

This work was supported by the Russian Foundation for Basic Research (grants 14-04-32001, 15-04-02185, 18-04-00120, and 18-04-00278). The study of the structure of the stand canopy was performed using TLS Leica ScanStation C10 form the Research Resource Center "Technical laboratory of ecology and ecophysiology" (Botanical Garden-Institute, Far Eastern Branch of the Russian Academy of Sciences).

Appendix A

See Figs. A1–A10 and Tables A1–A3

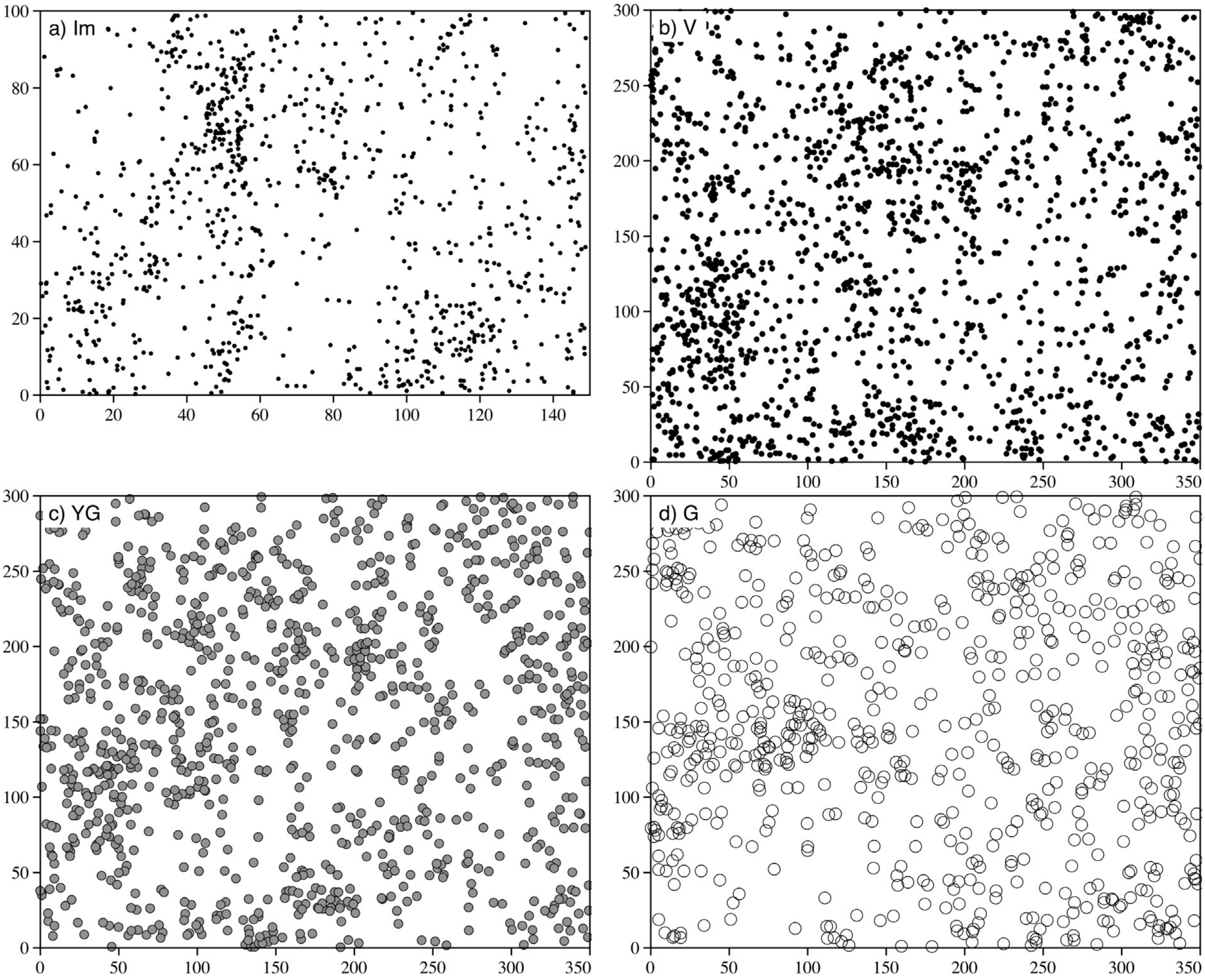

Fig. A1. Spatial distribution of *Abies nephrolepis* plants within the 1.5-ha (a) and 10.5-ha (b–d) permanent sample plots: (a) immature plants (im_1, im_2, im_3), (b) virginal plants (v_1, v_2), (c) young generative plants (v_3, g_1), (d) middle- and old-generative plants (g_2, g_3).

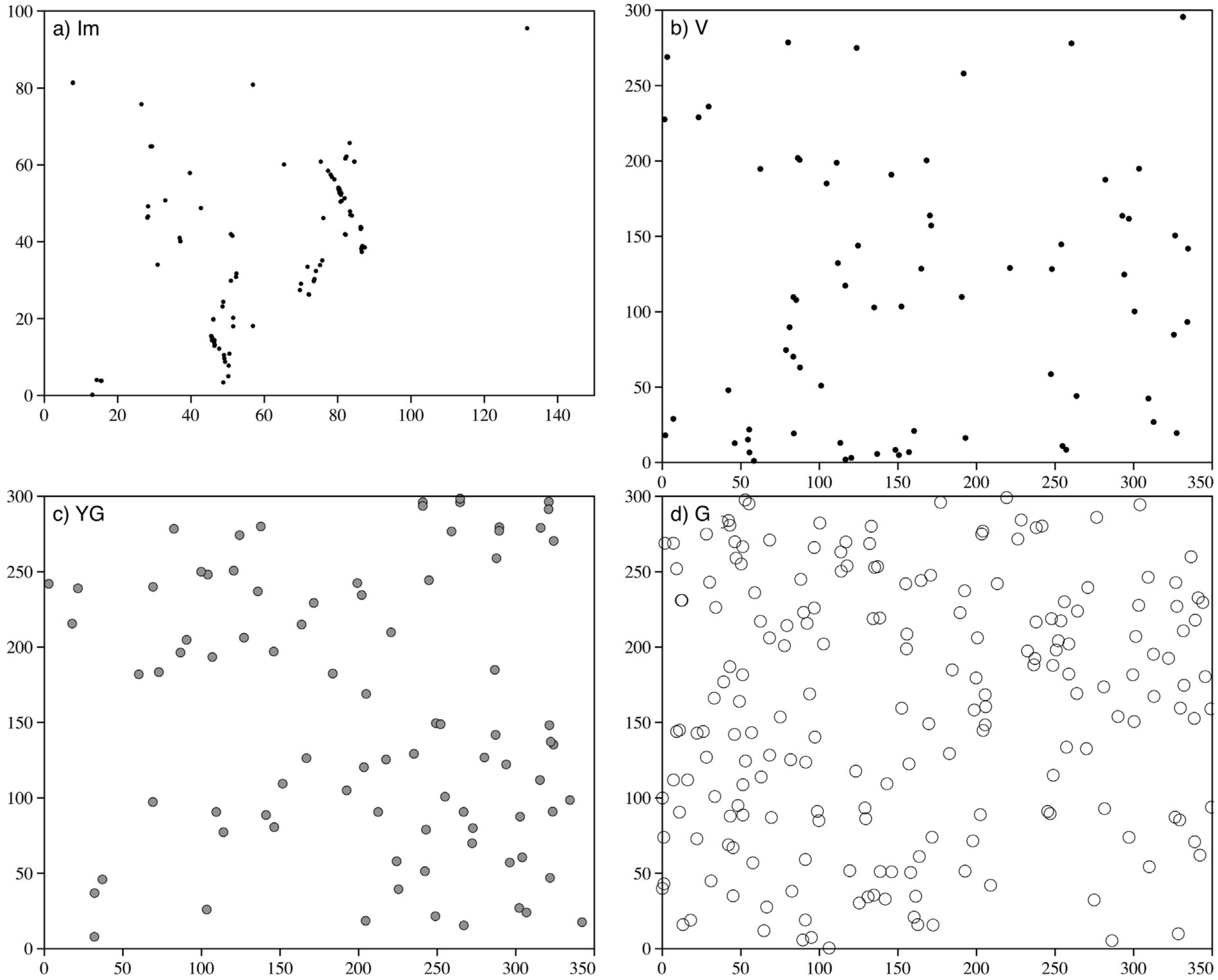

Fig. A2. Spatial distribution of *Betula costata* plants within the 1.5-ha (a) and 10.5-ha (b–d) permanent sample plots: (a) immature plants (im_1, im_2, im_3), (b) virginal plants (v_1, v_2), (c) young generative plants (v_3, g_1), and (d) middle- and old-generative plants (g_2, g_3).

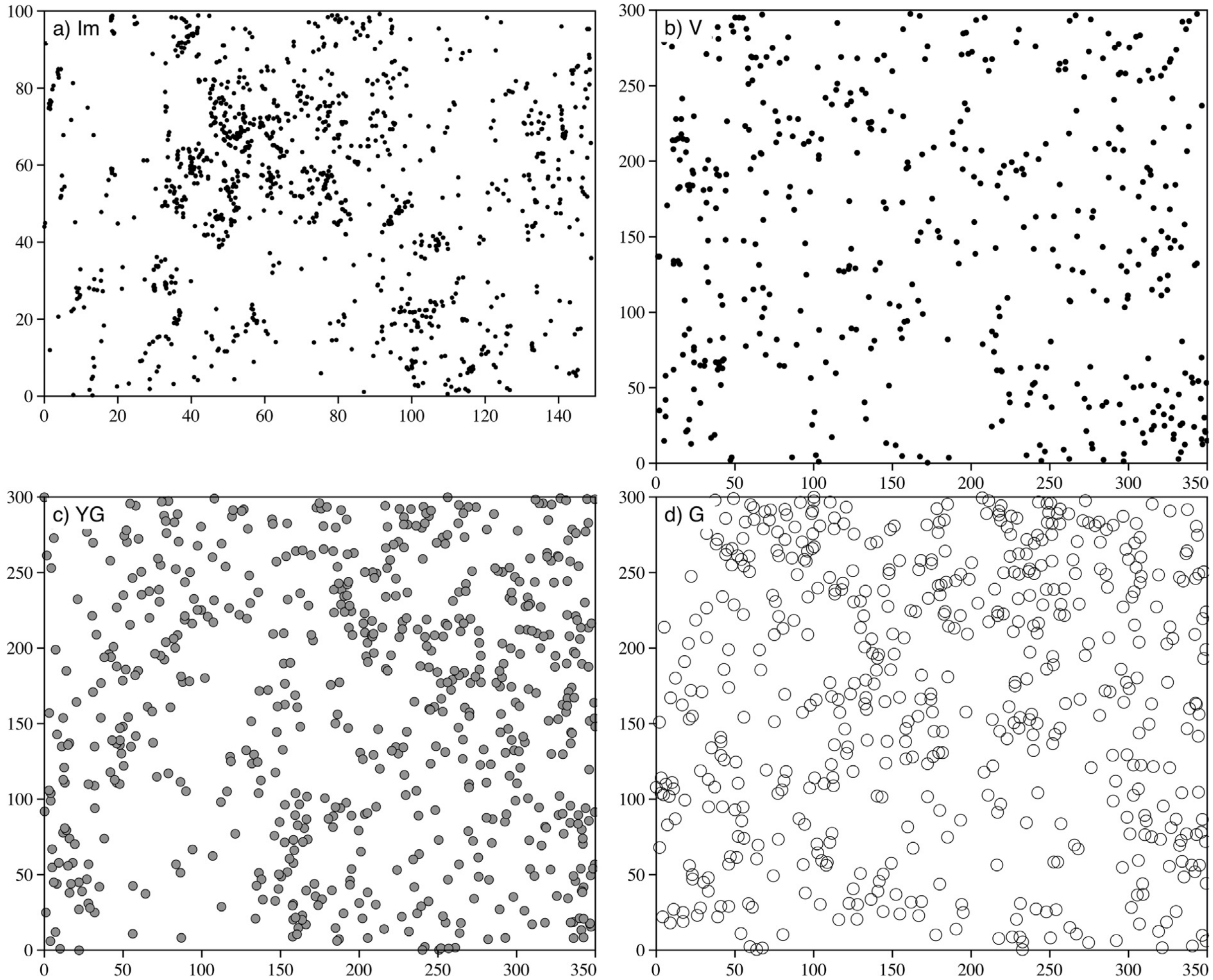

Fig. A3. Spatial distribution of *Picea jezoensis* plants within the 1.5-ha (a) and 10.5-ha (b–d) permanent sample plots: (a) immature plants (im_1, im_2, im_3), (b) virginal plants (v_1, v_2), (c) young generative plants (v_3, g_1), and (d) middle- and old-generative plants (g_2, g_3).

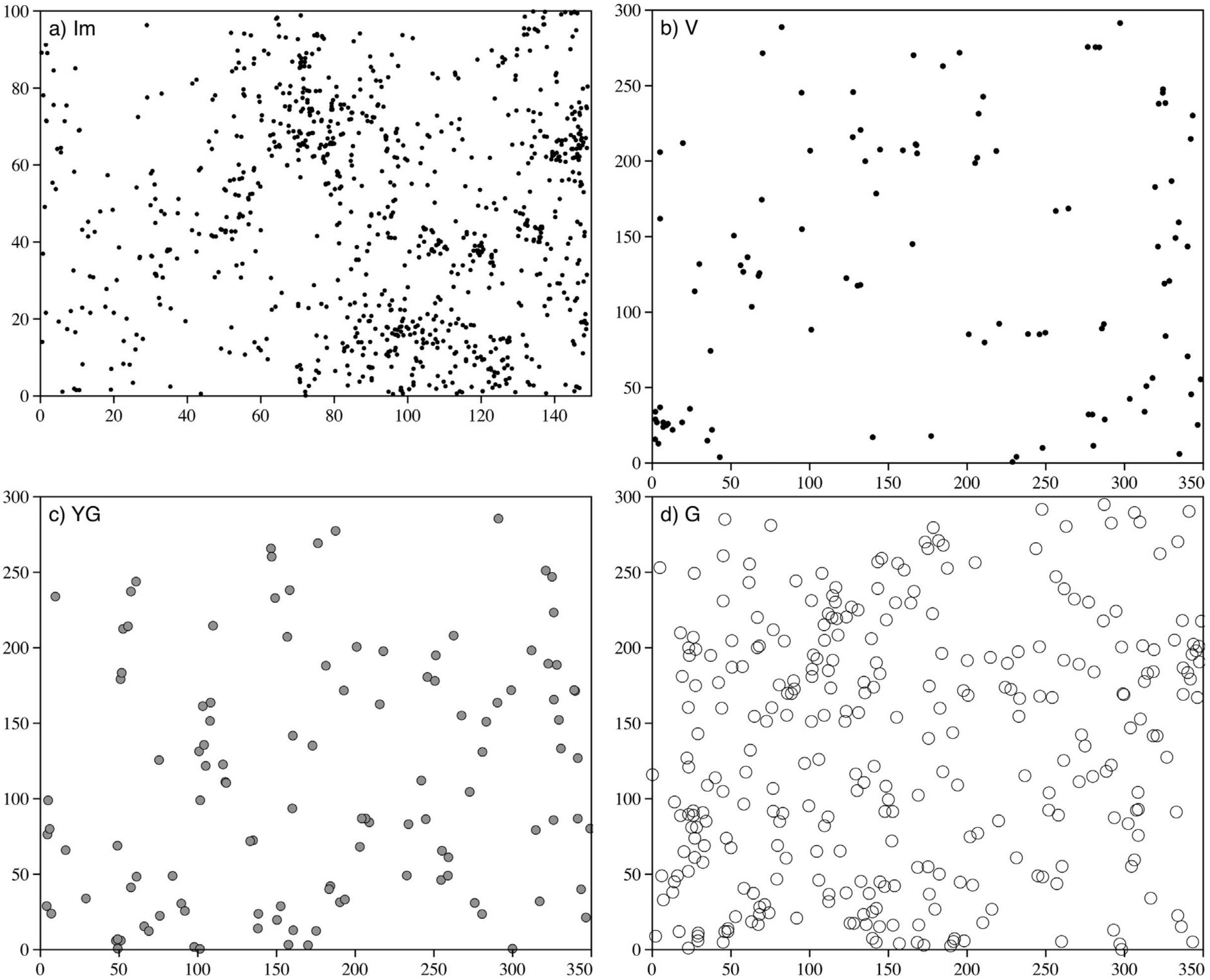

Fig. A4. Spatial distribution of *Pinus koraiensis* plants within the 1.5-ha (a) and 10.5-ha (b–d) permanent sample plots: (a) immature plants (im_1, im_2, im_3), (b) virginal plants (v_1, v_2), (c) young generative plants (v_3, g_1), and (d) middle- and old-generative plants (g_2, g_3).

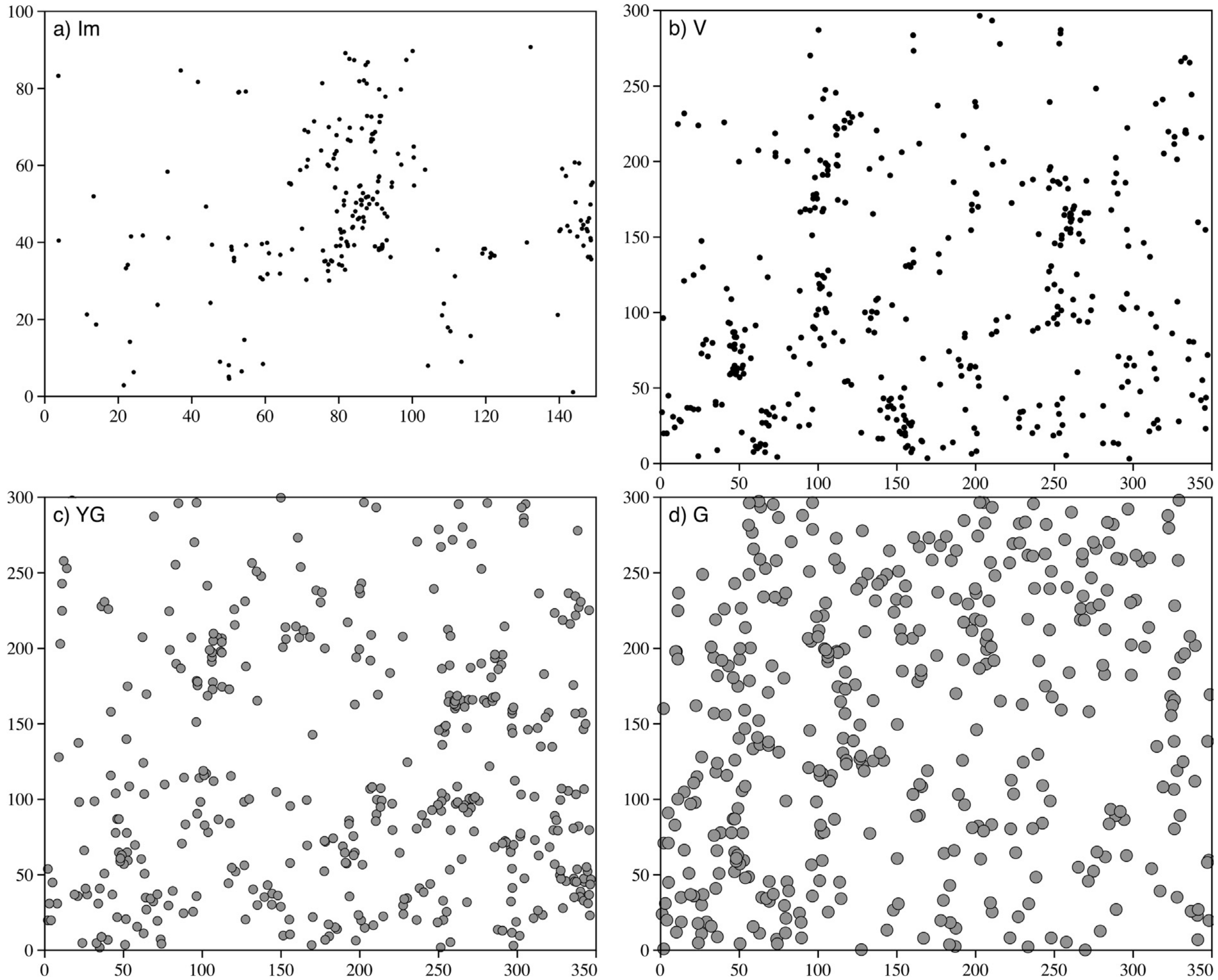

Fig. A5. Spatial distribution of *Tilia amurensis* plants within the 1.5-ha (a) and 10.5-ha (b–d) permanent sample plots: (a) immature plants (im_1, im_2, im_3), (b) virginal plants (v_1, v_2), (c) young generative plants (v_3, g_1), and (d) middle- and old-generative plants (g_2, g_3).

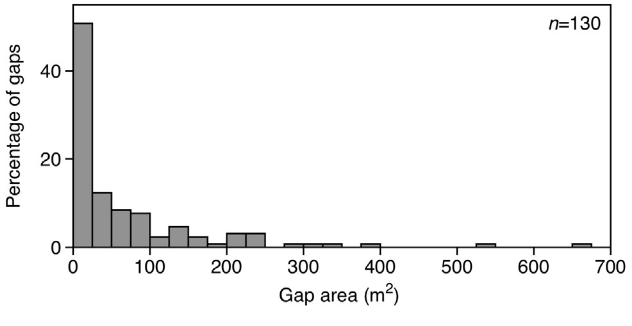

Fig. A6. Distribution of the canopy gap sizes on the 6-ha part of the 10.5-ha permanent sample plot.

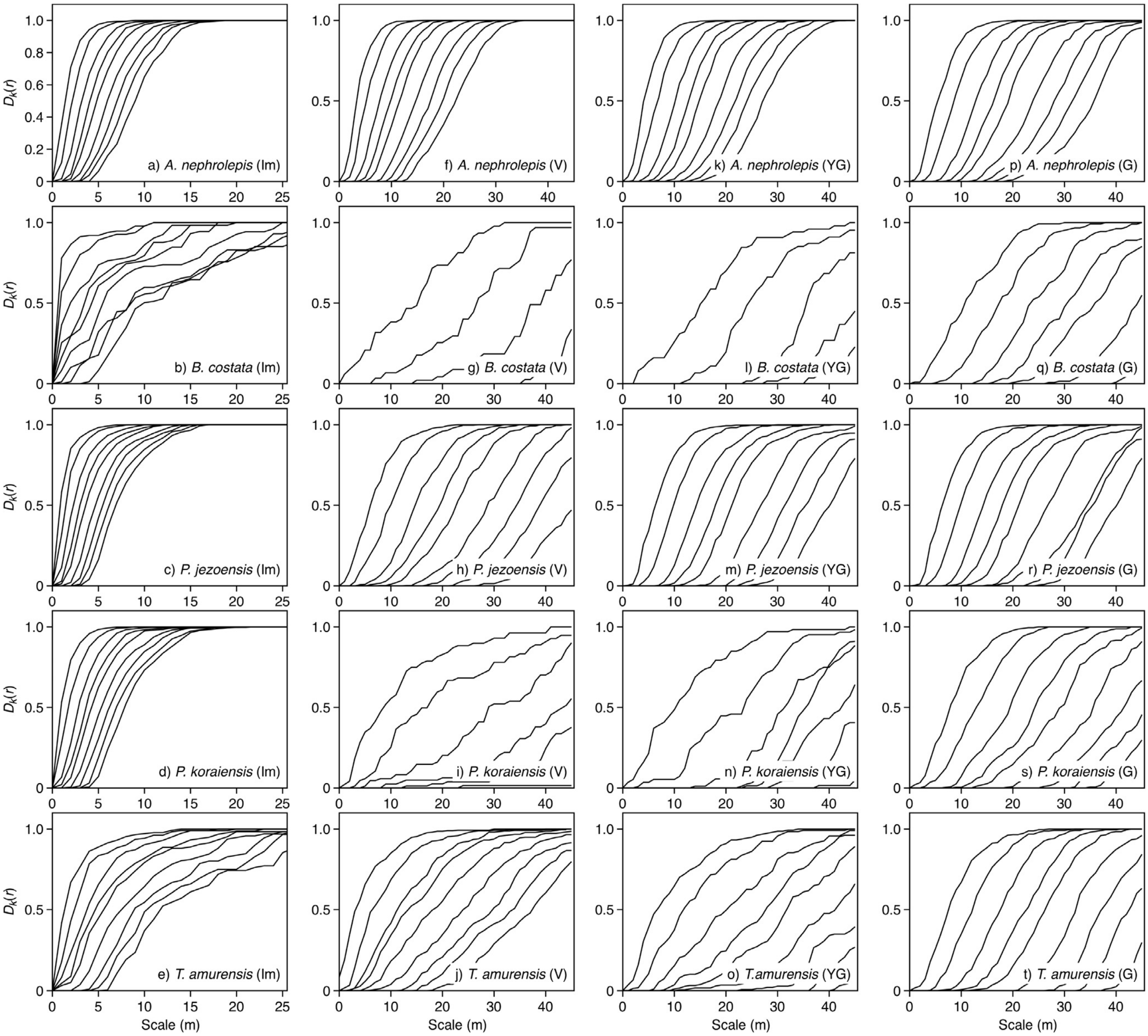

Fig. A7. Distribution of distances to the *k*th nearest neighbor ($k = 1, 2, 4, 6, 8, 12, 16, 20, 25$) in plant patterns of five dominated species. The insets show the analyses of point patterns of different ontogeny stages: Im - immature plants (im_1, im_2, im_3), V - virginal plants (v_1, v_2), YG – young generative plants (v_2, g_1), G - middle- and old-generative plants (g_1, g_2).

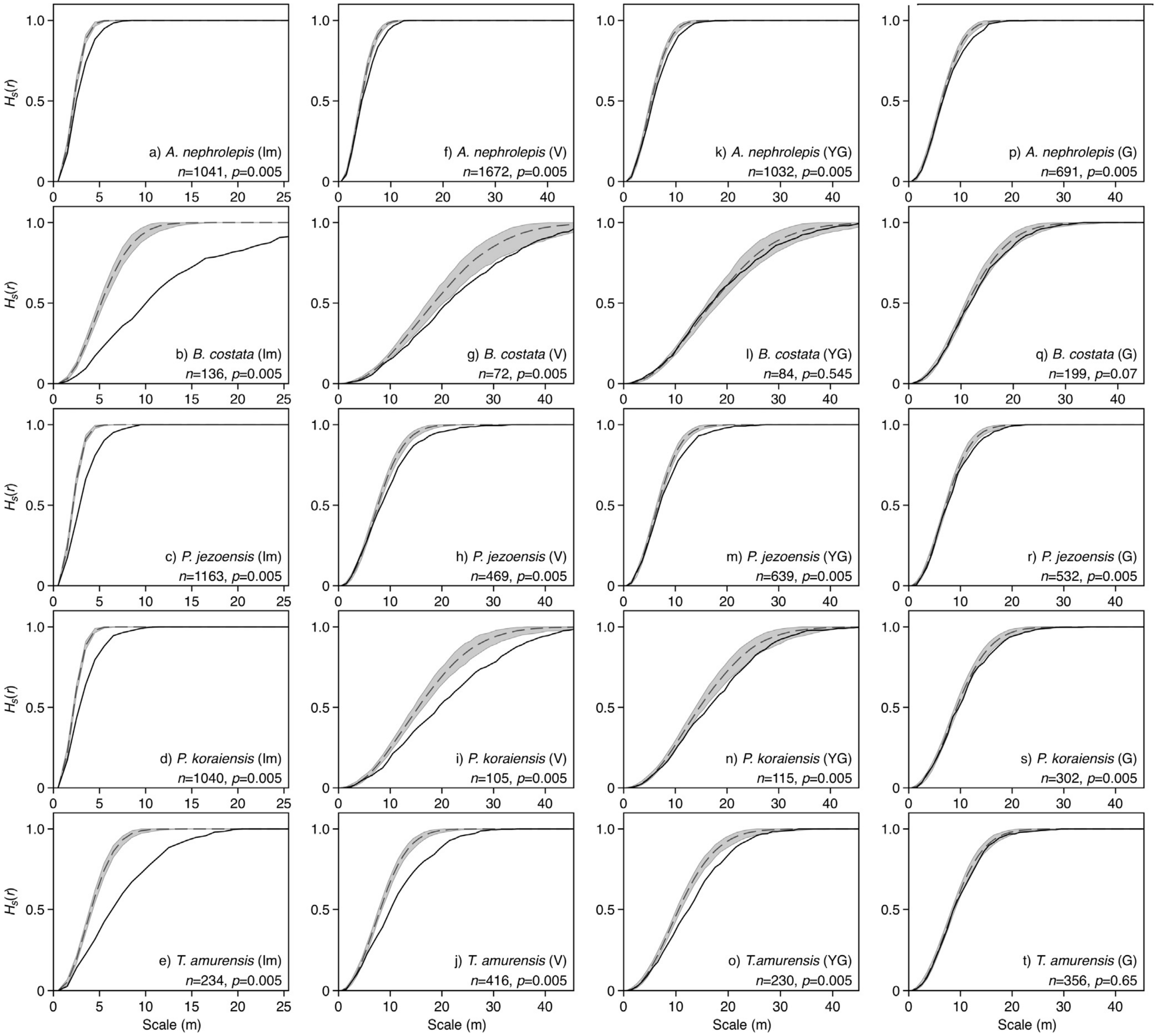

Fig. A8. Univariate point pattern analyses of five dominated tree species using spherical contact distribution function H_s. The insets show the analyses of point patterns of different ontogeny stages: Im - immature plants (im_1, im_2, im_3), V - virginal plants (v_1, v_2), YG – young generative plants (v_2, g_1), G - middle- and old-generative plants (g_1, g_2).

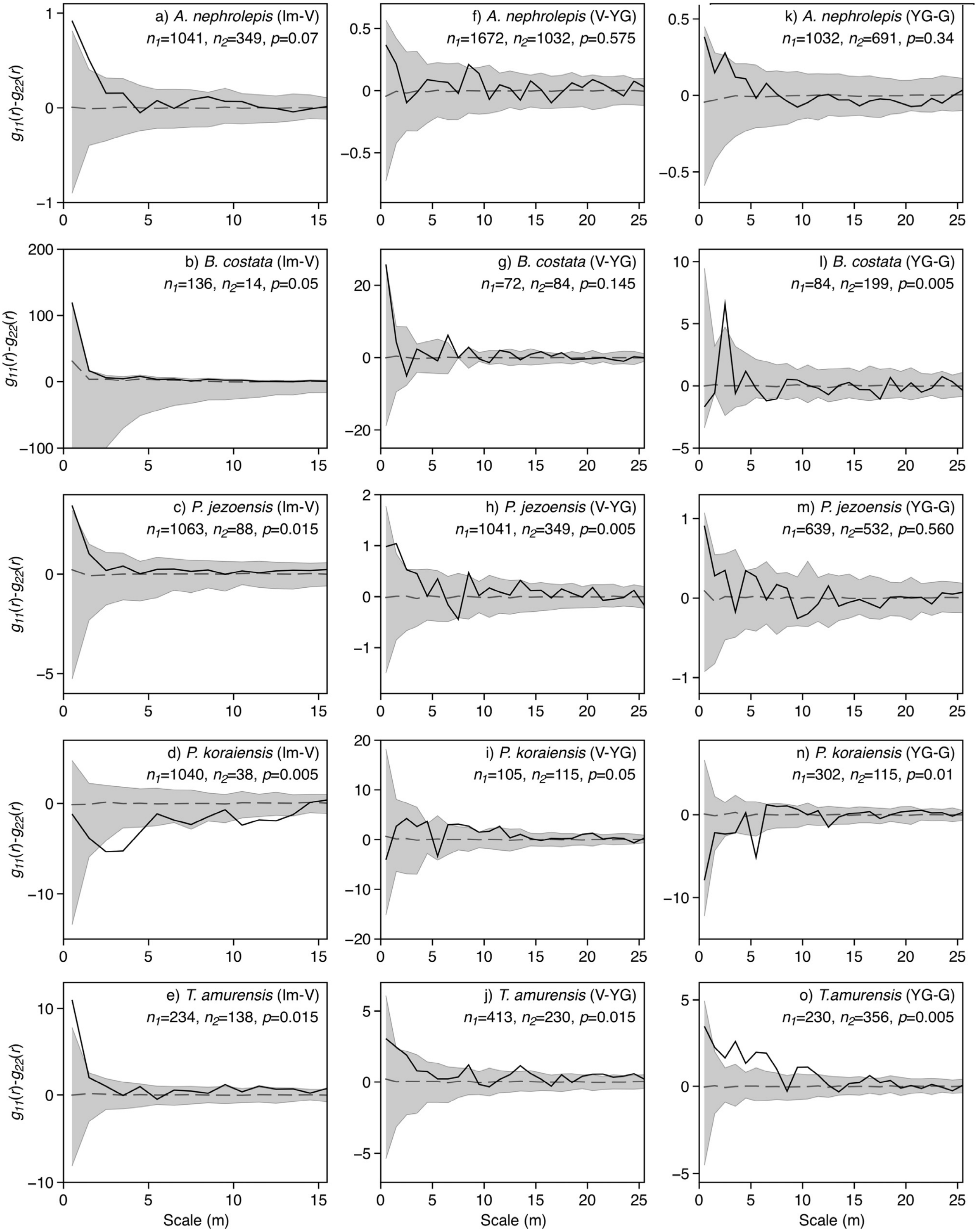

Fig. A9. Differences of the pair-correlation functions for patterns of plants in different ontogenetic stages: Im - immature plants (im_1, im_2, im_3), V - virginal plants (v_1, v_2), YG – young generative plants (v_2, g_1), G - middle- and old-generative plants (g_1, g_2). Solid line indicates the empirical curve, dashed line indicates the expected value under the null-model CSR, gray area indicates limits of 99% simulation envelope; n_1 *and* n_2 is number of plants and p is p-value of the GoF test.

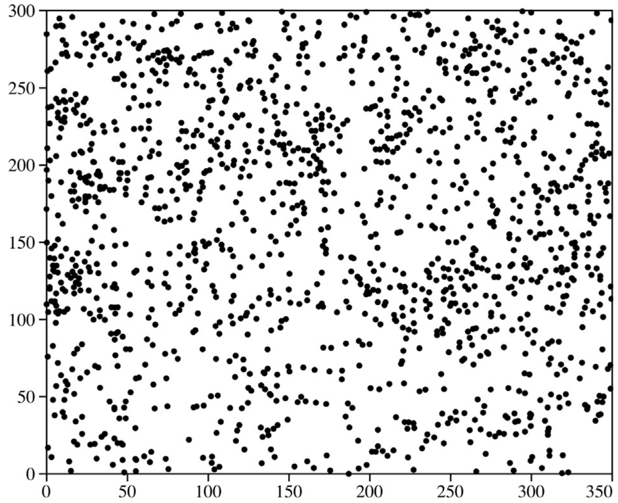

Fig. A10. Spatial distribution of stumps (middle-aged and old generative plants) within the 10.5-ha permanent sample plot.

Table A1
Characteristics of plants of five dominated species in different ontogenetic stages. H is plant height, H_c is height of crown beginning, R_c is crown radius, the dash denotes the lack of data (for DBH in means that plants height is less than 1.3 m).

Ontogenetic stage	Age (year)		DBH ± SD (cm)	H ± SD (m)	H_c ± SD (m)	R_c ± SD (m)
	min	max				
Abies nephrolepis						
Immature, phase 1 (im_1)	6	–	–	0.28 ± 0.10	0.15 ± 0.05	0.20 ± 0.15
Immature, phase 2 (im_2)	–	–	0.85 ± 0.45	0.94 ± 0.39	0.44 ± 0.22	0.98 ± 0.66
Immature, phase 3 (im_3)	–	121	3.93 ± 1.44	2.90 ± 0.40	1.92 ± 0.44	1.5 ± 0.48
Virginal, phase 1 (v)	30	129	5.77 ± 0.88	4.29 ± 0.43	3.29 ± 3.17	1.30 ± 0.26
Virginal, phase 2 (v_2)	44	123	7.90 ± 1.42	6.47 ± 1.05	4.04 ± 1.30	1.58 ± 0.33
Virginal, phase 3 (v_3)	47	149	12.00 ± 2.22	10.09 ± 1.55	5.99 ± 1.85	1.84 ± 0.34
Young reproductive (g_1)	75	151	16.24 ± 3.70	13.68 ± 1.97	8.72 ± 2.62	1.99 ± 0.48
Mature reproductive (g_2)	67	166	20.40 ± 4.21	17.56 ± 2.97	9.8 ± 2.69	2.04 ± 0.48
Old reproductive (g_3)	116	214	30.00 ± 7.04	22.74 ± 4.76	13.23 ± 2.95	2.39 ± 0.48
Betula costata						
Immature, phase 1 (im_1)	1	–	–	0.13 ± 0.06	–	–
Immature, phase 2 (im_2)	–	–	–	0.37 ± 0.02	–	–
Immature, phase 3 (im_3)	–	43	–	0.84 ± 0.28	–	0.2 ± 0.1
Virginal, phase 1 (v)	41	60	1.1 ± 0.5	1.7 ± 0.5	1.3 ± 0.3	1.5 ± 0.2
Virginal, phase 2 (v_2)	31	72	2.7 ± 1.4	4.4 ± 1.4	4.0 ± 1.2	1.3 ± 0.2
Virginal, phase 3 (v_3)	46	78	8.8 ± 3.2	10.4 ± 4.4	8.5 ± 3.4	1.5 ± 0.5
Young reproductive (g_1)	51	120	25.6 ± 2.9	19.5 ± 0.5	12.0 ± 1.6	3.4 ± 1.4
Mature reproductive (g_2)	85	282	43.9 ± 6.8	23.5 ± 2.9	15.0 ± 1.9	4.4 ± 1.1
Old reproductive (g_3)	258	340	60.2 ± 9.7	22.8 ± 8.3	13.3 ± 3.4	5.3 ± 1.1
Picea jezoensis						
Immature, phase 1 (im_1)	2	–	–	0.33 ± 0.14	–	0.24 ± 0.29
Immature, phase 2 (im_2)	–	–	1.24 ± 0.41	1.03 ± 0.39	0.55 ± 0.25	0.63 ± 0.41
Immature, phase 3 (im_3)	–	110	2.79 ± 0.69	2.50 ± 0.29	1.37 ± 0.39	1.61 ± 0.85
Virginal, phase 1 (v)	28	125	4.82 ± 1.68	4.04 ± 0.99	2.34 ± 1.14	1.38 ± 0.33
Virginal, phase 2 (v_2)	33	201	8.34 ± 1.8	6.84 ± 1.19	4.63 ± 1.64	1.66 ± 0.37
Virginal, phase 3 (v_3)	45	251	13.91 ± 2.79	12.47 ± 2.92	8 ± 2.63	2.03 ± 0.46
Young reproductive (g_1)	56	269	22.7 ± 3.47	19.736 ± 2.09	13.008 ± 2.09	2.48 ± 0.28
Mature reproductive (g_2)	65	317	28.25 ± 5.59	22.91 ± 2.08	13.5 ± 1.52	2.60 ± 0.56
Old reproductive (g_3)	87	277	33.74 ± 5.27	24.26 ± 1.66	13.6 ± 1.72	3.54 ± 0.45
Pinus koraiensis						
Immature, phase 1 (im_1)	6	–	–	0.44 ± 0.18	0.24 ± 0.09	0.18 ± 0.01
Immature, phase 2 (im_2)	–	–	1.43 ± 0.52	1.20 ± 0.42	0.50 ± 0.24	0.45 ± 0.23
Immature, phase 3 (im_3)	–	107	3.14 ± 1.13	3.13 ± 0.63	1.78 ± 0.76	1.85 ± 0.9
Virginal, phase 1 (v)	48	141	5.55 ± 1.73	4.42 ± 0.68	2.47 ± 0.85	1.09 ± 0.13
Virginal, phase 2 (v_2)	47	192	9.52 ± 2.95	8.29 ± 1.99	5.74 ± 2.39	1.33 ± 0.31
Virginal, phase 3 (v_3)	74	180	14.46 ± 5.84	12.20 ± 3.92	7.44 ± 2.87	1.65 ± 0.50
Young reproductive (g_1)	79	281	19.68 ± 7.79	16.40 ± 4.87	9.35 ± 3.54	2.46 ± 0.56
Mature reproductive (g_2)	158	303	45.85 ± 13.07	23.15 ± 7.26	13.02 ± 3.54	3.25 ± 0.78
Old reproductive (g_3)	242	527	60.56 ± 9.56	29.52 ± 4.63	16.78 ± 4.59	3.99 ± 0.76

(*continued on next page*)

Table A1 (*continued*)

Ontogenetic stage	Age (year)		DBH ± SD (cm)	H ± SD (m)	H_c ± SD (m)	R_c ± SD (m)
	min	max				
Tilia amurensis						
Immature, phase 1 (im_1)	13	–	–	0.16 ± 0.11	–	0.27 ± 0.19
Immature, phase 2 (im_2)	–	–	–	0.69 ± 0.22	–	0.75 ± 0.48
Immature, phase 3 (im_3)	–	37	–	0.54 ± 0.24	–	0.86 ± 0.37
Virginal, phase 1 (v)	22	45	3.90 ± 1.19	3.20 ± 0.89	2.39 ± 0.67	0.92 ± 0.14
Virginal, phase 2 (v_2)	28	46	6.21 ± 1.34	6.75 ± 1.75	5.14 ± 1.33	1.46 ± 0.37
Virginal, phase 3 (v_3)	35	60	11.12 ± 3.69	11.64 ± 2.06	7.27 ± 2.22	2.06 ± 0.51
Young reproductive (g_1)	58	161	20.52 ± 2.33	16.33 ± 2.17	9.32 ± 2.95	3.31 ± 0.85
Mature reproductive (g_2)	105	235	38.98 ± 7.33	21.17 ± 2.30	12.27 ± 2.72	4.14 ± 0.97
Old reproductive (g_3)	120	250	57.38 ± 9.17	23.72 ± 2.22	10.34 ± 3.09	4.92 ± 1.13

Table A2
General characteristics of plants of different vitality.

Vitality	Characteristics of plants
Normal	Usually occurs under optimal conditions; plant has maximal size and biomass; size and biomass increments strongly correlate with the calendar age until the senile ontogenetic stage
Subnormal	A plant has smaller size compared to the normal one; residuals of dying tops are visible on the trunk
Low (suppressed)	A plant has minimal size and biomass and grows very slowly; treetop frequently dies off; and the crown has many dead branches

Table A3
Frequencies of plants of normal (Norm.), subnormal (Sub.) and low (Low) vitality in different positions relative to canopy and gaps.

Species	Vitality	Immature (im_1, im_2, im_3)			Virginal (v_1, v_2)			Young generative (v_3, g_1)		
		Gap	Periphery	Canopy	Gap	Periphery	Canopy	Gap	Periphery	Canopy
A. nephrolepis	Norm.	50	54	4	118	120	16	278	139	25
	Sub.	49	147	339	22	268	531	52	194	253
	Low	35	59	304	143	56	398	23	15	53
B. costata	Norm.	27	14	2	18	5	2	59	8	2
	Sub.	5	18	36	5	21	7	2	7	2
	Low	3	14	17	1	6	7	1	2	1
P. jezoensis	Norm.	35	23	1	11	4	1	94	31	5
	Sub.	59	98	455	24	66	80	75	121	153
	Low	23	57	412	24	62	197	19	48	93
P. koraiensis	Norm.	11	58	26	12	7	2	51	16	5
	Sub.	32	129	562	2	21	42	2	21	11
	Low	5	26	191	1	3	15	3	3	3
T. amurensis	Norm.	4	9	9	67	33	6	128	17	5
	Sub.	2	22	131	31	126	89	20	37	16
	Low	1	4	52	4	17	43	2	1	4

References

Brown, C., Law, R., Illian, J.B., Burslem, D.F.R.P., 2011. Linking ecological processes with spatial and non-spatial patterns in plant communities. J. Ecol. 99, 1402–1414.

Brzeziecki, B., Kienast, F., 1994. Classifying the life-history strategies of trees on the basis of the Grimian model. For. Ecol. Manag. 69, 167–187.

Caswell, H., 2001. Matrix Population Models: Construction, Analysis, and Interpretation. Sinauer Associates, Inc., Publishers, Sunderland, Massachusetts.

Chesson, P., 2000. Mechanisms of maintenance of species diversity. Annu. Rev. Ecol. Evol. Syst. 31, 343–366.

Connel, J.H., 1978. Diversity in tropical rain forest and coral reefs. Sci. 199, 1302–1310.

Do, T.V., Satob, T., Saitod, S., Kozana, O., Yamagawae, H., Nagamatsuf, D., Nishimurag, N., Manabeh, T., 2015. Effects of micro-topographies on stand structure and tree species diversity in an old-growth evergreen broad-leaved forest, southwestern Japan. Glob. Ecol. Conserv. 4, 185–196.

Diggle, P.J., 2003. Statistical Analysis of Spatial Point Patterns. Edward Arnold, London.

East-European Forests (Russia), 2004. Moskow. 1, 551 (In Russian).

Evstigneev, O.I., 1996. The relation of deciduous trees to light and water availability in link to structure of forest. Rus. J. For. Sci. 6, 26–35 (In Russian).

Evstigneev, O.I., Korotkov, V.N., 2016. Ontogenetic stages of trees: an overview. Rus. J. Ecosyst. Ecol. 1 (2), 1–31.

Garcia-Cervigon, A.I., Velazquez, E., Wiegand, T., Escudero, A., Olano, J.M., 2017. Colonization in Mediterranean old-fields: the role of dispersal and plant–plant interactions. J. Veg. Sci. 28 (3), 627–638.

Grime, J.P., 1979. Plant Strategies and Vegetational Processes. Willey, New York.

Hao, Z., Zhang, J., Song, B., Ye, J., Li, B., 2007. Vertical structure and spatial associations of dominant tree species in an old-growth temperate forest. For. Ecol. Manag. 252, 1–11.

Harms, K.E., Condit, R., Hubbell, S.P., Foster, R.B., 2001. Habitat associations of trees and shrubs in a 50-ha Neotropical forest plot. J. Ecol. 89, 947–959.

Hubbell, S.P., 2001. The Unified Neutral Theory of Biodiversity and Biogeography. Princeton University Press, Princeton.

Illian, J., Penttinen, A., Stoyan, H., Stoyan, D., 2008. Statistical Analysis and Modelling of Spatial Point Patterns. John Wiley & Sons, Ltd.

Ishikawa, Y., Krestov, P.V., Namikawa, K., 1999. Disturbance history and tree establishment in old-growth *Pinus koraiensis*-hardwood forests in the Russian Far East. J. Veg. Sci. 10, 439–448.

Ivanov, G.I., 1964. Soils of Primorsky Kray (Russia). Dalnevostochnoe knizhnoe izdatelstvo, Vladivostok (in Russian).

Jara-Guerrero, A., De la Cruz, M., Espinosa, C.I., Méndez, M., Escudero, A., 2015. Does spatial heterogeneity blur the signature of dispersal syndromes on spatial patterns of woody species? A test in a tropical dry forest. Oikos 000, 001–007.

John, R., Dalling, J.W., Harms, K.E., Yavitt, J.B., Stallard, R.F., Mirabello, M., Hubbell, S.P., Valencia, R., Navarrete, H., Vallejo, M., Foster, R.B., 2007. Soil nutrients influence spatial distributions of tropical tree species. Proc. Natl. Acad. Sci. USA 104, 864–869.

Kanagaraj, R., Wiegand, T., Comita, L.S., Huth, A., 2011. Tropical tree species assemblages in topographical habitats change in time and with life stage. J. Ecol. 99, 1441–1452.

Karpov, V.G., 1969. Experimental Phytocenology of Dark-Conifer Taiga. Nauka, Leningrad (In Russian).

Kenkel, N.C., 1988. Patterns of self-thinning in jack-pine: testing of the random mortality hypothesis. Ecology 69, 1017–1024.

Kolesnikov, B.P., 1956. Korean pine forests of the [Russian] Far East. Trudy DVF AN SSSR 2, 1–264 (in Russian).

Komarova, T.A., 1986. Regeneration by seed in fresh bums (forests of the Sourthen Sikhote-Alin). Dalnevostochnoe knizhnoe izdatelstvo, Vladivostok (in Russian).

Komarova, T.A., Trofimova, A.D., 2010. Stages of *Pinus koraiensis* (Pinaceae) ontogenesis in sourthen Sikhote-Alin. Veg. Resour. 4, 1–15 (in Russian).

Komarova, T.A., Ukhvatkina, O.N., Trofimova, A.D., 2010. Ontogenesis of Korean Pine (*Pinus koraiensis* Sieb. et Zucc.) in middle mountains of Sourthen Sikhote Aline (Russia). Bull. Bot. Gard.-Inst. FEB RAS 5, 81–92 (in Russian).

Kozhevnikova, N.K., 2009. Dynamics of weather-climatic characteristics and ecological function of small river basin. Sib. Ecol. J. 5, 693–703 (in Russian).

Krestov, P.V., 2003. Forest vegetation for Easternmost Russia (Russian Far East). For. Veg. Northeast Asia. Dordrecht. pp. 93–180.

Lai, J.S., Mi, X.C., Ren, H.B., Ma, K.P., 2009. Species-habitat associations change in a subtropical forest of China. J. Vet. Sci. 20, 415–423.

Liu, Y., Li, F., Jin, G., 2014. Spatial patterns and associations of four species in an old-growth temperate forest. J. Plant Interact. 9 (1), 745–753.

May, F., Huth, A., Wiegand, T., 2015. Moving beyond abundance distributions – neutral theory and spatial patterns in a tropical forest. Proc. R. Soc. B 282, 20141657.

Omelko, A.M., Ukhvatkina, O.N., 2012. Characteristics of gap-dynamics of conifer-broadleaved forest of Sourthen Sikhote-Alin (Russia). Plant World Asian Russ. 1, 106–113 (in Russian).

Omelko, A.M., Ukhvatkina, O.N., Zhmerenetsky, A.A., 2016. Disturbance history and natural regeneration of an old-growth Korean pine-broadleaved forest in the Sikhote-Alin mountain range, Southeastern Russia. For. Ecol. Manag. 360, 221–234.

Orekhova, T.P., 2005. Seeds of tree plants in Far East (Russia). Vladivostok (in Russian).

Petrenko, T.Y., Ukhvatkina, O.N., Omelko, A.M., Zhmerenetsky, A.A., 2016. Virginale plants development of *Picea ajnensis* (Lindl. et Gord.) Fisch. ex carr. in old-growth Korean pine-broadleaf forest in the territory of the Southern Sikhote-Alin. Bull. Irkutsk State Univ. Ser. Biol. Ecol. 18, 14–26 (in Russian).

Petrillo, M., Cherubini, P., Fravolini, G., Marchetti, M., Ascher-Jenull, J., Schärer, M., Synal, H.-A., Bertoldi, D., Camin, F., Larcher, R., Egli, M., 2016. Time since death and decay rate constants of Norway spruce and European larch deadwood in subalpine forests determined using dendrochronology and radiocarbon dating. Biogeosciences 13, 1537–1552.

Piao, T.F., Comita, L., Jin, G.Z., Kim, J.H., 2013. The importance of density dependence in regulating plant populations by acting cross multiple life-history stages. Oecologia 172, 207–217.

Punchi-Manage, R., Wiegand, T., Wiegand, K., Getzin, S., Gunatilleke, C.V.S., Gunatilleke, I.A.U.N., 2014. Effect of spatial processes and topography on structuring species assemblages in a Sri Lankan dipterocarp forest. Ecol. 95 (2), 376–386.

R Core Team, 2017. R: A Language and Environment for Statistical Computing. R Foundation for Statistical Computing, Vienna, Austria.

Schiffers, K., Schurr, F.M., Tiebörger, K., Urbach, C., Moloney, K.A., Jeltsch, F., 2008. Dealing with virtual aggregation - a new index for analysing heterogenous point pattern. Ecography 31, 545–555.

Seidler, T.G., Plotkin, J.B., 2006. Seed dispersal and spatial pattern in tropical trees. PLoS Biol. 4 (11), e344.

Shipley, B., Paine, C.E.T., Baraloto, C., 2012. Quantifying the importance of local niche-based and stochastic processes to tropical tree community assembly. Ecol. 93, 760–769.

Smirnova, O.V., 2004. Methodological approaches and methods of assessing climax and succession state of forest ecosystems (from the example of East European Forests). Rus. For. Sci. 3, 15–27 (in Russian).

Smirnova, O.V., Bobrovskii, M.V., 2001. Tree ontogeny and its reflection in the structure and dynamics of plant and soil covers. Russ. J. Ecol. 32, 159–163.

Stoyan, D., Stoyan, H., 1994. Fractals, Random Shapes and Point Fields. Methods of Geometrical Statistics. Wiley, New York.

Svoboda, M., Janda, P., Bace, R., Fraver, S., Nagel, T.A., Rejzek, J., Mikolas, M., Douda, J., Boubl, K., Samonil, P., Cada, V., Trotsiuk, V., Teodosiu, M., Bouriaud, O., Biris, A., Sykora, O., Uzel, P., Zelenka, J., Sedlak, V., Lehejcek, J., 2014. Landscape-level variability in historical disturbance in primary *Picea abies* mountain forests of the Eastern Carpathians, Romania. J. Veg. Sci. 2014 (25), 386–401.

Trostiuk, V., Svoboda, M., Janda, P., Mykolas, M., Base, R., Rejzek, J., Samonil, P., Chaskovskyy, O., Korol, M., Myklush, S., 2014. A mixed severity disturbance regime in the primary *Picea abies* (L.) Karst. For. Ukran. Carpath. For. Ecol. Manag. 334, 144–153.

Ukhvatkina, O.N., Komarova, T.A., Trofimova, A.D., 2010. Features of ontogenesis of *Picea ajanensis* (Lindl. et Gord.) Fisch. ex Carr. in middle mountain of southern Sikhote-Alin. J. Moscow State For. Univ. 3, 169–173 (in Russian).

Ukhvatkina, O.N., Omelko, A.M., 2016. Life strategy of the Korean pine (*Pinus koraiensis* Sieb. et Zucc.) in the old-growth Korean pine-broadleaved forest, Southern part of the Sikhote-Alin Mountain Range. Tomsk State Univ. J. Biol. 4 (36), 164–179 (in Russian).

Ukhvatkina, O.N., Omelko, A.M., Krestov, P.V., Zhmerenetsky, A.A., 2011. Impact of moderate disturbances on regeneration in Korean-pine forests. J. Sib. Fed. Univ. 4, 416–436 (in Russian).

Ukhvatkina, O.N., Omelko, A.M., Zhmerenetskiy, A.A., Gusev, V.S., 2015. Natural disturbances regime as a factor of Korean pine-broadleaved forest stand shaping in the south of the Russian Far East. J. Siberian Fed. Univ. Biol. 8 (4), 441–458 (in Russian).

Ukhvatkina, O.N., Omelko, A.M., Zhmerenetsky, A.A., Petrenko, T.Ya., 2017. Formation of the spatial pattern of the *Picea ajanensis* (Pinaceae) population in the Korean pine-broadleaved forest on the south of the Russian Far East. Rastitelnye resursy 53 (1), 70–87 (in Russian).

Usenko, N.V., 1968. Trees, Shrubs and Lianas in Far East (Russia). Khabarovsk (in Russian).

Wang, X.G., Ye, J., Li, B.H., Zhang, J., Lin, F., Hao, Z.Q., 2010. Spatial distributions of species in an old-growth temperate forest, northeastern China. Can. J. For. Res. 40 (6), 1011.

Wiegand, T., He, F., Hubbell, S.P., 2013. A systematic comparison of summary characteristics for quantifying point patterns in ecology. Ecography 36 (1), 92–103.

Wiegand, T., Moloney, K.A., 2014. Handbook of Spatial Point-Pattern Analysis in Ecology. CRC Press, London, New York.

Wright, S.J., 2002. Plant diversity in tropical forests: a review of mechanisms of species coexistence. Oecologia 130, 1–14.

Zhang, J., Hao, Z.Q., Li, B.H., Ye, J., Wang, X.G., Yao, X.L., 2008. Composition and seasonal dynamics of seed rain in Broad-leaved Korean pine mixed forest, Changbai Mountain. Acta Ecol. Sin. 28, 2245–2254.

Zhang, J., Song, B., Li, B.-H., Ye, J., Wang, X.-G., Hao, Z.-Q., 2010a. Spatial patterns and associations of six congeneric species in an old-growth temperate forest. Acta Oecol. 36, 29–38.

Zhang, L., Mi, X., Shao, H., Ma, K., 2011. Strong plant-soil associations in a heterogeneous subtropical broad-leaved forest. Plant Soil 347, 211–220.

Zhang, Y., Drobyshev, I., Gao, L., Zhao, X., Bergeron, Y., 2014. Disturbance and regeneration dynamics of a mixed Korean pine dominated forest on Changbai Mountain, North-Eastern China. Dendrochronologia 32, 21–31.

Zhang, Z.H., Hu, G., Zhu, J.D., Luo, D.H., Ni, J., 2010b. Spatial patterns and interspecific associations of dominant tree species in two old-growth karst forests, SW China. Ecol. Res. 25 (6), 1151.